The human ABCG1 gene: identification of LXR response elements that modulate expression in macrophages and liver

Steven L. Sabol,[1] H. Bryan Brewer, Jr., and Silvia Santamarina-Fojo

Molecular Disease Branch, National Heart, Lung, and Blood Institute, National Institutes of Health, Bethesda, MD 20892

Abstract **The ABC transporter ABCG1 (ATP binding cassette transporter G1), expressed in macrophages, liver, and other tissues, has been implicated in the efflux of cholesterol to high density lipoprotein. The ABCG1 gene is transcriptionally activated by cholesterol loading and activators of liver X receptors (LXRs) and retinoid X receptors (RXRs) through genomic sequences that have not been fully characterized. Here we show that ABCG1 mRNA is induced by LXR agonists in RAW264.7 macrophage cells, HepG2 hepatoma cells, and primary mouse hepatocytes. We identify two evolutionarily highly conserved LXR response elements (LXREs), LXRE-A and LXRE-B, located in the first and second introns of the human ABCG1 gene. Each element conferred robust LXR-agonist responsiveness to ABCG1 promoter-directed luciferase gene constructs in RAW264.7 and HepG2 cells. Overexpression of LXR/RXR activated the ABCG1 promoter in the presence of LXRE-A or LXRE-B sequences. In gel-shift assays, LXR/RXR heterodimers bound to wild-type but not to mutated LXRE-A and LXRE-B sequences. In chromatin immunoprecipitation assays, LXR and RXR were detected at LXRE-A and -B regions of DNA of human THP-1 macrophages. These studies clarify the mechanism of transcriptional upregulation of the ABCG1 gene by oxysterols in macrophages and liver, two key tissues where ABCG1 expression may affect cholesterol balance and atherogenesis.**—Sabol, S. L., H. B. Brewer, Jr., and S. Santamarina-Fojo. **The human ABCG1 gene: identification of LXR response elements that modulate expression in macrophages and liver. *J. Lipid Res.* 2005.** 46: **2151–2167.**

Supplementary key words ATP binding cassette transporter • liver X receptor • retinoid X receptor • cholesterol • hepatocyte • oxysterols • T-0901317 • promoter • transcription start site

The ATP binding cassette transporter G1 (ABCG1) is a member of a large superfamily of evolutionarily conserved transmembrane proteins that transport a variety of molecules across membranes. Many of the approximately 48 known human ABC transporters, which are divided into seven families (A–G), have been implicated in disease (1, 2). ABCG1, originally termed "White" and "ABC8" (3–5), is a half-transporter (74–76 kDa) possessing one ATP binding/hydrolysis cassette and one transmembrane domain and is presumed to form dimers or multimers with either itself or another half-transporter to assemble a functional complex (6). ABCG1 mRNA is expressed at high or moderate levels in macrophages, spleen, lung, thymus, placenta, brain, and fetal tissues, and at lower levels in most other tissues, including liver (3–5, 7–9).

Recent studies have implicated ABCG1 in the cellular transport and efflux of cholesterol and possibly phospholipids. Klucken et al. (10) first demonstrated that treatment of human macrophages with antisense oligonucleotides targeting ABCG1 mRNA resulted in decreased efflux of cholesterol and phospholipids to HDL_3, a major fraction of high density lipoprotein (HDL). More recently, Wang et al. (11) and Nakamura et al. (12) reported that increased expression of ABCG1 or the closely related transporter ABCG4 in human embryonic kidney cells increased cholesterol efflux to HDL. Other studies have shown that overexpressing ABCG1 in mouse hepatocytes via adenovirus infection reduced plasma HDL levels and increased cholesterol secretion into bile, findings consistent with a role for ABCG1 in the transport of cholesterol in liver cells (13, 14). Furthermore, green-fluorescent protein-tagged human ABCG1 protein in HeLa cells was found to be localized in endocytic compartments and the plasma membrane, consistent with a role for ABCG1 in intracellu-

Manuscript received 25 February 2005 and in revised form 7 July 2005.

Published, JLR Papers in Press, July 16, 2005.
DOI 10.1194/jlr.M500080-JLR200

Abbreviations: ABCG1, ATP-binding cassette transporter family G member 1; Ac-LDL, acetyl low density lipoprotein; 9cRA, 9-*cis*-retinoic acid; DR4, direct repeat with four intervening nucleotides; EMSA, electrophoretic mobility shift assay; LXR, liver X receptor; LXRE, LXR response element; 22-OH-cholesterol, 22(*R*)-hydroxycholesterol; RACE, rapid amplification of cDNA ends; RXR, retinoid X receptor; Nucleotide abbreviations: R, A or G; Y, C or T; M, A or C; K, G or T; n, any base.

[1] To whom correspondence should be addressed.
e-mail: slsabol@mail.nih.gov

lar sterol trafficking as well as efflux (15). These combined findings suggest a role for ABCG1, as yet undefined, in reverse cholesterol transport, the process whereby excess cholesterol is removed from cells, transported to the liver, and excreted into bile (16).

As might be anticipated, ABCG1 gene expression is highly regulated by cholesterol. ABCG1 mRNA levels in cultured mouse and human macrophages were highly induced by lipid loading with acetyl low density lipoprotein (Ac-LDL) (10, 17, 18) and reduced by lipid depletion (10). Furthermore, the normally low level of ABCG1 mRNA in rat liver parenchymal cells was increased 4-fold by feeding a high-cholesterol diet (9). These combined data suggest sterol-mediated regulation of ABCG1 gene expression in macrophages, which are important in the initiation of atherosclerosis and, in liver, the major tissue involved in cholesterol homeostasis.

Lipid loading or a high-cholesterol diet stimulates reverse cholesterol transport through the activation of the liver X receptor (LXR) transcriptional pathway (19–21). The LXR nuclear receptors LXRα and LXRβ form obligate heterodimers with retinoid X receptors (RXRs) and bind naturally occurring oxidized cholesterol derivatives such as 24(*S*),25-epoxycholesterol, 22(*R*)-, 24(*S*)-, and 27-hydroxycholesterol (18, 21–24) and synthetic nonsteroidal compounds such as T-0901317 (25). RXR receptors bind the agonist 9-*cis*-retinoic acid (9cRA) (26). LXR/RXR heterodimers recognize an LXR response element (LXRE) sequence containing a variant direct-repeat-4 (DR4) motif in the promoters and introns of several genes affecting lipid metabolism (22, 27, 28). The binding of a ligand for either LXR or RXR can activate the heterodimer submaximally to stimulate transcription, whereas ligands for both receptors are required for maximal activation (29). The LXR/RXR heterodimer is normally bound to a corepressor or coactivator protein in the absence or presence of agonists, respectively (30–32).

LXR activation dramatically increases ABCG1 mRNA levels in macrophages (17, 33). Venkateswaran et al. (17) demonstrated that the inducibility of ABCG1 mRNA levels by oxysterols was retained in macrophages from mice lacking either of the two LXR receptor genes but was lost in mice lacking both genes, indicating that either LXRα or LXRβ can activate the ABCG1 gene. More recently, treatment of mice with T-0901317 has been shown to elevate markedly ABCG1 mRNA levels in several tissues, including liver, macrophages, and adipose tissue (12, 34, 35). LXR activation also strongly activates transcription of the gene for the important cholesterol/phospholipid transporter ABCA1, which stimulates efflux to circulating apolipoprotein A-I (19, 20, 36, 37). By the activation of the ABCA1, ABCG1, and other genes, the LXR pathway is critical to the regulation of cholesterol homeostasis, as well as the prevention of cholesterol accumulation in macrophages leading to atherosclerosis (19, 21, 33).

The human ABCG1 gene on chromosome 21q22.3 is relatively expansive and subject to alternative RNA splicing (38–40). The major transcript is derived from 15 exons spanning a region of 78.1 kb (38). Its promoter region is highly GC-rich and lacks a TATA box; furthermore, the transcription start site(s) have not been adequately determined previously. Efforts to find a functional LXRE in the promoter and upstream region of the human ABCG1 gene have been unsuccessful (41). Kennedy et al. (40) reported two putative LXREs in the second intron[2] of the human gene; however, these sequences are not conserved in the mouse and rat ABCG1 genes. Very recently, Nakamura et al. (12) published preliminary evidence for a different set of LXREs in the second intron of the mouse ABCG1 gene. Vertebrate genomes are now known to contain regions of evolutionarily conserved sequence far from exons and promoters that regulate gene transcription over large distances (42–44). Adopting this perspective in the present study, we have employed evolutionary conservation as a criterion for identifying potentially functional and important LXREs in and near the human ABCG1 gene. We report the characterization of two novel, robustly active, and evolutionarily conserved LXREs (LXRE-A and LXRE-B) in the first and second introns[2] of the human ABCG1 gene and demonstrate their functionality in cultured macrophage and hepatic cell lines. These studies enhance our understanding of the mechanisms by which oxysterols upregulate human ABCG1 transcription in two key tissues, liver and macrophages, where changes in ABCG1 expression and cellular cholesterol efflux may markedly alter cholesterol balance and atherogenesis.

MATERIALS AND METHODS

Materials

T-0901317 (25) was purchased from Cayman Chemical Co. (Ann Arbor, MI). 22(*R*)-hydroxycholesterol (22-OH-cholesterol) and 9cRA were from Sigma (St. Louis, MO). Stock solutions were dissolved in 95% ethanol. Human genomic DNA and total RNA from placenta and liver were from Clontech (Palo Alto, CA).

Analyses of ABCG1 mRNA in cell lines

RAW264.7 mouse macrophage and HepG2 human hepatoma cells [American Type Culture Collection (ATCC); Manassas, VA] were maintained in Dulbecco's modified Eagle's medium (DMEM) containing 10% fetal bovine serum. For mRNA studies, cells were grown in 75 cm^2 flasks until 60–70% confluency was reached. The medium was changed to serum-free DMEM containing 1 mg/ml BSA, and the cells were treated with LXR/RXR agonist drug(s) or vehicle for 12 h. All experimental conditions were tested in triplicate flasks. Total RNA was isolated using Trizol reagent (Invitrogen; Carlsbad, CA) as instructed by the manufacturer. Ten micrograms RAW264.7 total RNA/lane were electrophoresed on a 1% agarose gel, blotted onto ZetaProbe GT mem-

[2] To prevent confusion and to facilitate cross-species comparison, in this study, we number human ABCG1 exons and introns according to the table of Langmann et al. (38), which lists exons of the originally described and apparently major ABCG1 mRNA transcript (GenBank accessions BC029158, NM_004915, and NM_016818) initiated at the promoter shown in Fig. 2. Transcripts initiating at this promoter actually consist of two alternatively spliced isoforms differing by the presence or absence of 36 coding bases, because of the presence of two alternate splice donor sites at the end of exon 9 (4).

branes (Bio-Rad; Hercules, CA), and probed with a ^{32}P-labeled 252 bp DNA corresponding to bases 1,052–1,303 of the mouse ABCG1 cDNA sequence in GenBank accession NM_009593, using standard methods for Northern blotting. Radioactive bands were visualized, quantitated on a phosphorimager (model 445SI; Molecular Dynamics, Sunnyvale, CA), and normalized to intensities of cyclophilin mRNAs obtained after rehybridizing the blot with a probe for mouse cyclophilin A (Ambion; Austin, TX, #7375). ABCG1 mRNA in HepG2 cells was detected by RT-PCR of first-strand cDNA prepared from total RNA using SuperScript II reverse transcriptase (Invitrogen). The forward and reverse PCR primers were GCCACTTTCGTGGGCCCAGTGA and TCTCATCACCAGCTGTGTTGCA, which amplifies a 658 bp sequence within exons 14–15 (bases 1,763–2,420 in GenBank accession BC029158). Touchdown PCR reactions containing Taq polymerase and 1 μl of cDNA synthesis reaction were carried out at annealing temperatures of 63°C, 61°C, and 59°C for 5 cycles each, followed by 57°C for 25 cycles. Aliquots (12.5 μl) were analyzed on a 1.2% agarose gel containing 0.5 μg/ml ethidium bromide and photographed in a ChemiImager 5500 (Alpha Innotech; San Leandro, CA).

Isolation and ABCG1 mRNA analysis of primary hepatocytes

Livers of 3-month-old C57Bl/6 male mice were perfused through the vena cava and common bile duct with 3–4 ml of Liver Perfusion Medium (Invitrogen/Gibco, #17701) followed by 4–8 ml of a solution containing 7.5 mg/ml collagenase Type 1 (Worthington; Lakewood, NJ, #LS004196) and 10 μl/ml protease inhibitor cocktail (Sigma, #P8340) in Hanks balanced saline solution (Gibco, #14175) supplemented with 10 mM $CaCl_2$/10 mM Hepes (Gibco #15630) at 37°C. The liver was dispersed by mincing and trituration in a large-bore pipette, and the suspension was passed through a nylon cell strainer (100 μm pore; BD-Falcon #352360, BD-Bioscience, Bedford, MA). Hepatocytes were separated from smaller liver cell types by washing with Hepatocyte Wash Medium (Gibco, #17704) followed by centrifugations at 50 *g* for 5 min five to six times, after which the cells were judged by light microscopy to be entirely (>99.5%) hepatocytes. The isolated, washed hepatocytes were plated in 6-well poly-lysine-coated plates (BD-BioCoat, #354413) at a density of 10^6 cells/well in DMEM/F12 (Gibco, #11039) supplemented with penicillin-streptomycin-glutamine and 10% fetal bovine serum. Cells were treated with 1 μM T-0901317 and/or 10 μM 9cRA, or solvent alone (ethanol, final 0.2%) for 16 h.

Total RNA was isolated using the Ultraspec-RNA reagent (Biotecx; Houston, TX) according to the manufacturer's instructions. For Northern blot analysis, approximately 5 μg of total RNA per lane were electrophoresed and hybridized with the mouse ABCG1 cDNA probe, and subsequently with the mouse cyclophilin A probe, as described above for cell lines. The densities of the major ABCG1 mRNA band were quantitated with ChemiImager 5500 software and normalized to cyclophilin A mRNA band intensities, and independently to 18S and 28S rRNA band intensities.

5′-rapid amplification of cDNA ends and RNase protection analyses

Transcription start sites were determined by 5′-rapid amplification of cDNA ends (RACE) through use of the Smart RACE cDNA Amplification Kit (Clontech). The gene-specific primer was TGGAGTGCCTTCGGGTCGCGAAGAGGAG, which is complementary to bases 176–203 of the coding sequence of human ABCG1 in exon 2,[2] where base 1 is the A of the ATG coding for the most upstream in-phase Met. Total RNA from human placenta, spleen, thymus, and fetal brain (Clontech), as well as THP-1 cells treated with 22-OH-cholesterol and 9cRA, was used for cDNA synthesis. Touchdown PCR reactions contained Taq polymerase and a cosolvent additive PCRx Enhancer (Invitrogen, final concentration 2–2.5×). Annealing temperatures were 68°C, 66°C, and 64°C for 5 cycles each, followed 60°C for 30 cycles. Amplification of all cDNAs tested resulted in a heterogeneous band at 370–410 bp with a sharp midpoint at 390 bp. The most robust amplification was with placental cDNA. RACE products from placental cDNA were cloned into the pCR2.1-TOPO vector (Invitrogen), and inserts from 30 clones were sequenced.

RNase protection experiments were performed using standard procedures (45). A template for antisense RNA synthesis was prepared by amplification of DNA of the main ABCG1 promoter and 5′-untranslated regions corresponding to bases −651 to −48 relative to the ABCG1 translation start site, using a reverse primer having a 5′-terminal T7 RNA polymerase promoter sequence. ^{32}P-labeled antisense RNA was prepared and annealed to total RNA from untreated or 22-OH-cholesterol/9cRA-treated THP-1 macrophages. Pancreatic and T1 RNase digestions were performed under varied conditions, and protected fragments were analyzed by polyacrylamide gel electrophoresis and autoradiography. Lengths of bands consistently protected by RNA from LXR/RXR-treated cells but not by RNA from untreated cells were used to map transcription factor start sites.

Genomic sequence analyses

Repeat-masked human and mouse genomic sequences were aligned by use of the Web-based mVISTA program (http://www.gsd.lbl.gov/VISTA/) (46, 47). Identification of putative transcription factor binding sites was made by use of the Web-based MatInspector program (Genomatix Software; Munich, Germany, http://www.genomatix.de/) (48) and the Web-based rVISTA program (http://www.gsd.lbl.gov/VISTA/) (49), which employed Transfac Pro v6.2 matrices.

The human genome sequence information is from the May 2004 assembly (hg17, NCBI build 35) (50). Sequences resembling human LXRE regions in the ABCG1 genes of other vertebrate genomes were obtained from publicly available draft assemblies generated by the following consortia: Chimpanzee Genome Sequencing Consortium, the Whitehead/Broad Institutes of MIT and Harvard and Agencourt Bioscience (dog genome), the Broad Institute (laboratory opossum genome), the Mouse Genome Sequencing Consortium (51), the Rat Genome Project at the Baylor College of Medicine Human Genome Sequencing Center (52), the Cow Genome Sequencing Consortium at the Baylor College of Medicine Human Genome Sequencing Center (http://www.hgsc.bcm.tmc.edu), the International Chicken Genome Sequencing Consortium (53), and Genoscope and the Broad Institute (*Tetraodon nigroviridis* genome (54)). Multispecies genome alignments can be visualized on the UCSC Genome Browser (http://genome.ucsc.edu) (55, 56). For other species, we used the BLAST tool to find similar sequences from raw DNA sequence trace archives at the National Center for Biotechnology Information website (http://www.ncbi.nlm.nih.gov/blast/index.shtml).

Construction of reporter plasmids

Plasmid reporter constructs containing the ABCG1 5′-untranslated region, the major promoter ["promoter B" (39)], and varied amounts of upstream region were prepared by insertion of a nested set of genomic sequences into the *Kpn*I and *Nhe*I sites of the promotorless pGL3-Basic vector (Promega; Madison, WI). The genomic sequences were amplified from human genomic DNA. Forward primers consisted of *Kpn*I site-tagged sequences at varied upstream sites of the sense (coding) strand of the ABCG1 gene. The common reverse primer (GAGAAAGCGGCCATCAGACAGCTAGCGCCC) contained the antisense strand sequence corresponding to bases −4 to +26 (numbered relative to the A of the initiating ATG defined as 1), except for the substitution of a *Nhe*I site for the bases coding for the initiating Met and the sec-

ond amino acid Ala. PCR reactions contained Pfx polymerase and 2.5× PCRx Enhancer (both from Life Technologies/Invitrogen) and standard components. Amplified DNA was digested with *Kpn*I and *Nhe*I and ligated into pGL3-Basic. The resulting plasmids possess the ABCG1 regulatory promoter and 5′-untranslated sequences in the sense orientation placed just upstream from the reporter firefly luciferase coding sequence. These constructs were named pGL3-hABCG1(−x/+123), where bases −x and +123 are the most upstream and downstream bases, respectively, of the insert, numbered in relation to the main ABCG1 transcription start site determined by us by 5′-RACE, which is 123 bases upstream from the ATG translation initiation start site (Fig. 2).

Intronic DNA sequences were tested for LXR responsiveness by cloning them into the *Sal*I site downstream of the firefly luciferase gene of the plasmid pGL3-hABCG1(−1,013/+123), whose preparation is described above. Some test sequences were also cloned into the *Kpn*I site of pGL3-hABCG1(−1,013/+123) just upstream from the regulatory promoter. The extended 287 bp LXRE-A region (chr21:42,513,461-42,513,747) with *Sal*I or *Kpn*I ends was obtained by PCR amplification of human genomic DNA. A clone containing base substitutions in the DR4 sequence of the LXRE-A region (1–287) were created by the use of the Quik-Change II Site-Directed Mutagenesis Kit (Stratagene; La Jolla, CA) essentially according to the manufacturer's protocol; the mutated DR4 sequence was AGGTAACTGTCtGatc, where mutated bases are shown in lowercase type. Inserts of mutant clones were sequenced, and an insert having the desired sequence was recloned into unamplified *Sal*I-cut pGL3-hABCG1(−1,013/+123), to eliminate any PCR misincorporations within the vector. The LXRE-B region (47 bp, chr21:42,528,054-42,528,100) and human LXRE-C region (47 bp, chr21:42,521,372-42,521,418) with *Sal*I or *Kpn*I ends and with or without mutations in the DR4 sequence were prepared as synthetic complementary oligodeoxynucleotides and cloned. The mutated LXRE-B and LXRE-C DR4 sequences were GcGaTtCTACCtGagA and AGGTTACTGTAtGatc, respectively, where mutated bases are shown in lowercase type. Unless otherwise indicated, clones selected for transfection studies possessed tested sequences oriented so that the strand appearing in the UCSC Genome Browser as the "upper strand" (the sense strand of human ABCG1 exons) was placed on the strand having the sense sequence of the luciferase gene. The tested 48 bp mouse LXRE-C region (chr17:29,673,084-29,673,131, May 2004 mouse genome assembly) corresponded in sequence alignment to the tested 47 bp human LXRE-C region and was cloned into the *Sal*I site as an oligodeoxynucleotide duplex. Clones having either one copy or two tandem copies of the mouse LXRE-C region, all in the "reverse" orientation to that defined above, were isolated and tested.

Clones possessing truncated portions of the LXRE-A region were generally prepared by PCR amplification of selected regions with primers containing *Sal*I sites, followed by ligation into the *Sal*I site of pGL3-hABCG1(−1,013/+123). Exceptions were the 52 bp fragments from base 79 to base 131, which were prepared by annealing of complementary oligodeoxynucleotides with protruding *Sal*I ends.

The sequences of the inserts were confirmed by DNA sequencing. All plasmids used in transfections were purified by use of the Endo-Free Plasmid Maxi Kit (Qiagen; Valencia, CA) or by two cycles of CsCl-ethidium chloride density gradient centrifugation.

Transfections and luciferase analyses

RAW264.7 cells (3–5 × 10^5/well) or human HepG2 cells (2 × 10^5/well) were plated in 12-well dishes containing 1 ml medium/well, unless otherwise indicated. All experimental conditions were tested in quadruplicate wells. On the day after plating cells, each well received a solution (100 μl) containing 1 μg test plasmid with the firefly luciferase reporter gene, 0.050 μg pRL-SV40 DNA (Promega) with the *Renilla* luciferase reporter gene to control for variations in transfection efficiency and cell number, 3 μl Fugene 6 reagent (Roche, Indianapolis, IN), and PBS. Approximately 24 h later, the cells were washed twice with PBS, and the medium was changed to serum-free DMEM containing 1 mg/ml BSA. LXR and RXR agonist compounds in ethanol were added as indicated (final ethanol concentration 0.2%). After 24 h, cells were washed twice with PBS, lysed in Passive Lysis Buffer (Promega) supplemented with Protease Inhibitor Cocktail (Sigma), and assayed by the Dual Luciferase Assay kit (Promega) in a MicroLumat Plus LB 96V luminometer (Berthold USA; Oak Ridge, TN) according to the kit manual (2–5 μl and 20 μl lysate/test for HepG2 and RAW264.7 lysates, respectively). The average expression level of the *Renilla* luciferase in transfected cells was not consistently affected by LXR and RXR agonists. Results were expressed as the ratio of firefly to *Renilla* light units multiplied by 10 for convenience (mean ± SEM, n = 4). Statistical significance was determined by use of the unpaired two-tailed Student's *t*-test.

Construction and expression of plasmids encoding LXR and RXR proteins

Plasmids containing the complete coding sequences for human LXRα (22), LXRβ (57), and RXRα (58) under the control of T7 and CMV promoters were constructed in the vector pcDNA3.1 (Invitrogen). RefSeq sequences (GenBank NM_005693, NM_007121, and NM_002957, respectively) were used to design PCR primers to amplify full-length coding sequences and insert a *Not*I site and consensus Kozak sequence (CCACC) immediately upstream from the ATG translation start site and to insert a second stop codon (TAA) and *Xba*I site immediately after the native stop codon. RT-PCR was performed with Pfu Ultra HF polymerase (Stratagene), PCRx Enhancer (final concentration 2×; Invitrogen), and cDNA from fetal human liver (for LXRα and RXRα) and placenta (for LXRβ). Amplicons were digested with *Not*I and *Xba*I and ligated into pcDNA3.1. Clone inserts were completely sequenced in both strands. Insert sequences of all clones containing LXRα cDNA differed from the RefSeq sequence at three bases but agreed at these positions with the reference human genome sequence and with other human LXRα cDNA sequences in GenBank. Insert sequences for LXRβ and RXRα cDNA were in complete agreement with the RefSeq sequences. The plasmids (termed "pcDNA-LXRα," "pcDNA-LXRβ," and "pcDNA-RXRα") were used as templates for LXR and RXR protein synthesis in the TNT T7 Quick Coupled Transcription/Translation kit (Promega) according to the manufacturer's instructions; template-minus reactions were also prepared.

Electrophoretic mobility shift assays

Double-stranded 28 bp oligodeoxynucleotide probes containing the following DR4 sequences (with direct repeats in bold face) were prepared by annealing complementary single-stranded oligodeoxynucleotides and were end-labeled with [γ-^{32}P]ATP (3,000 Ci/mmol; Perkin-Elmer, Boston, MA) and T4 polynucleotide kinase (Invitrogen) and purified on G-25 spin columns:

LXRE-A-wt: GGCAAG**AGGTAA**CTGT**CGGTCA**AATCCT
LXRE-A-mut: GGCAAG**AGGTAA**CTGT**Ct**G**G**atcAATCCT
LXRE-B-wt: GCGCCG**GGGTTA**CTAC**CGGTCA**ACGCTC
LXRE-B-mut: GCGCCG**G**c**G**a**T**tCTAC**Ct**G**G**ag**A**ACGCTC
hLXRE-C-wt: CACACA**AGGTTA**CTGT**AGGGCA**AGTCTC
mLXRE-C-wt: CTACAG**AGGTTA**CTAC**AGGGCA**AACAGC
LXRE-A-50: CTCTTGAGCTCAAGGCAAG**AGGTAA**CTGT**CGGTCA**AATCCTGCTGAGCCC
LXRE-A-50-centro: GGCAAG**AGGTAA**CTGT**CGGTCA**AATCCTGCTGAGCCCTGCTGACTTCAAA
LXRE-A-50-telo: TTTTTTTTCTCTTGAGCTCAAGGCAAG**AGGTAA**CTGT**CGGTCA**AATCCTT

Gel shift binding reaction mixtures (10 μl final volume) contained (as indicated in figure legends) either 0.5–1 μl cell-free transcription/translation reaction mixture for each receptor tested or 1 μg RAW264.7 cell nuclear extract (59) (Paragon Bioservices; Baltimore, MD), as well as 20 mM Tris HCl (pH 7.9), 60 mM KCl, 1.3 mM $MgCl_2$, 0.2 mM EDTA, 0.5 mM dithiothreitol, 10% glycerol, 3% Ficoll, 50 μg/ml poly dI:poly dC, and 20,000 cpm ^{32}P-labeled probe (2,500–5,000 cpm/fmol, added last). Incubations were for 10 min at room temperature followed by an additional 10 min on ice. For competition assays, unlabeled double-stranded probe in molar excess over the labeled probe was added and incubated with the receptors and buffer for 3 min prior to addition of the probe. In supershift assays, 4 μg immunoglobulin G (IgG) antibodies (Santa Cruz Biotechnology; Santa Cruz, CA) were preincubated for 10 min at room temperature with reaction mixtures prior to addition of the probe. The samples were loaded onto 6% polyacrylamide nondenaturing gels containing 0.5 × Tris-borate-EDTA (TBE) buffer (Invitrogen) and electrophoresed at 100 V for 30 min followed by 130 V for 1.5 h. The gels were dried and analyzed by a phosphorimager.

Chromatin immunoprecipitation (ChIP) assay

THP-1 human monocyte cells (ATCC) were maintained in RPMI-1640 medium with 10% fetal bovine serum and were differentiated by treatment with 50 nM phorbol myristate acetate (PMA) for 48–72 h. The medium was changed to serum-free RPMI-1640 with 1% BSA, and cultures were treated with 1 μM T-0901317 plus 5 μM 9cRA, or solvent (ethanol) alone, for 90–120 min. The ChIP-IT kit (Active Motif; Carlsbad, CA) and accompanying protocol were used for subsequent steps. Briefly, the cells were fixed with 1% formaldehyde for 10 min at room temperature. Nuclei were isolated and sonicated on ice to shear the chromatin to fragments of 200–1,200 bp (average 500 bp). ChIP reactions (4°C, overnight) contained precleared unfrozen chromatin (50 μg protein or 8 μg DNA from 1.2–1.5 × 10^6 cells) and 3 μg of rabbit IgG. Protein G-agarose beads (100 μl, preblocked additionally with 1 mg/ml sonicated herring sperm DNA) were added, and the beads were subsequently washed extensively. Bound chromatin was eluted with 1% SDS at 60°C for 10 min and purified on spin columns supplied with the kit.

The recovered DNA was assayed for sequences closely surrounding LXRE DR4 motifs by PCR reactions (25 μl) containing 3 μl ChIP DNA (or 3–5 ng DNA isolated from each chromatin preparation), Platinum *Taq* polymerase (Invitrogen), and the following pairs of forward and reverse primers to amplify sequences of indicated lengths: LXRE-A, CCGAGGCTGTAAGCCCACAGT, GCGGAGCATGCGCAGAAACCT, 183 bp; LXRE-B, CTCAACGCCCGGGAGAAAACAG, CTCCGCCGCGGAGGTTACTA, 164 bp; LXRE-C, AGTGAGGGAGGAGCCCCAACT, ACCCCTCTGGCTCCACCCATTT, 170 bp. The PCR program consisted of 32–34 cycles of 94°C for 25 s, 58°C for 30 s, and 72°C for 30 s. Reactions for amplification of the LXRE-B sequence required cosolvent (1.75× PCRx Enhancer; Invitrogen) because of its high GC content. Amplification products were electrophoresed on a 2.5% agarose gel containing 0.25% ethidium bromide and photographed.

RESULTS

LXR and RXR agonists upregulate ABCG1 gene expression in cultured macrophages, hepatoma cells, and primary hepatocytes

We evaluated potential LXREs using two well-differentiated cell lines, RAW264.7 mouse macrophage cells and HepG2 human hepatoma cells, which serve as model systems, with limitations, for normal macrophages and hepatic parenchymal cells (hepatocytes), respectively. Prior to transfection, we demonstrated that the endogenous ABCG1 gene in these cells and in primary mouse hepatocytes is responsive to LXR agonists. In RAW264.7 cells, we found by Northern blot analysis (**Fig. 1A**) that treatment with T-0901317 or 9cRA for 12 h increased the relative abundance of 3.8 kb full-length mature ABCG1 mRNA to 6.5 ± 0.7× and 3.4 ± 0.5× control, respectively, whereas treatment with both drugs increased the abundance to 8.1 ± 1.5× control (means ± SEM, n = 3, normalized to cyclophilin mRNA levels). In untreated and treated HepG2 cells, we could not detect ABCG1 mRNA by Northern analysis (data not shown). Nevertheless, as illustrated in Fig. 1B, we were able to consistently amplify ABCG1 cDNA prepared from RNA from HepG2 cells treated with T-0901317 ± 9cRA but not from cells treated with solvent alone, indicating that the levels of ABCG1 mRNA in HepG2 cells, although extremely low, are upregulated by LXR agonist. Our overall results are consistent with previous reports demonstrating induction of ABCG1 mRNA by oxysterols and 9cRA in RAW264.7 cells (17) and by oxysterols in HepG2 cells (60).

To further investigate the physiological relevance of the HepG2 findings with respect to the liver, we studied the induction of ABCG1 mRNA by T-0901317 and/or 9cRA in isolated primary mouse hepatocytes (Fig. 1C). By Northern analysis, a faint band at 3.8 kb consistent with mature full-length ABCG1 mRNA was detected in RNA from primary hepatocytes treated with solvent alone. Treatment of the cells with T-0901317 or 9cRA for 16 h increased its relative abundance to 6.1× and 1.6× control, respectively, whereas treatment with both drugs elicited an increase to 8.5× control (normalized to cyclophilin mRNA levels). These results demonstrate that ABCG1 mRNA in isolated primary hepatocytes, although normally low in abundance, is detectable and strongly upregulated by LXR agonist, with additional potentiation by RXR activation.

Identification of major transcription start sites

Previous attempts to identify the transcription start site(s) associated with the major human ABCG1 promoter [termed "promoter B" (39)] utilizing the 5′-RACE method were unsuccessful because of difficulty in amplifying the 5′-untranslated region, which contains a 49 bp GC-rich region including a $(CCG)_{10}$ repeat (38, 39). We used the independent methods of 5′-RACE, with an additive to destabilize GC-rich templates, and RNase protection. By the 5′-RACE method, we identified several apparent start sites, the major one of which was at base −123 relative to the first in-phase ATG translation start site (**Fig. 2**). More-distant but less-utilized start sites were found at bases −130, −140, and −146. By the RNase protection method, we found multiple bands of antisense RNA protected from digestion by annealing with RNA from LXR/RXR-agonist-treated THP-1 human macrophage cells (gel not shown). Most bands were in a cluster corresponding to start sites at base −116 to −121 relative to the translation start site (ac-

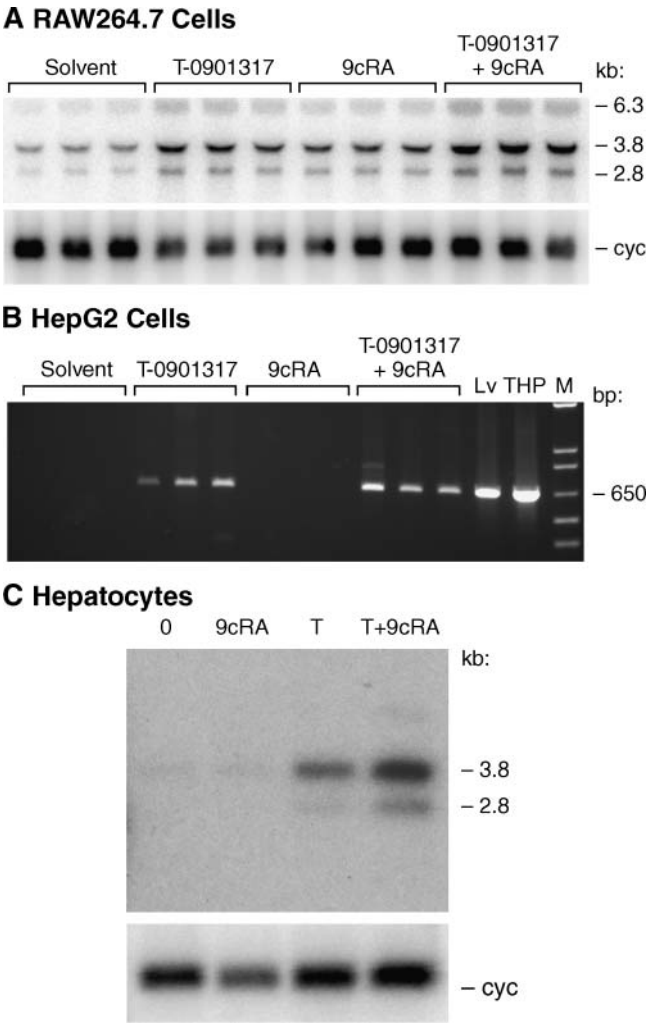

Fig. 1. Regulation of ABCG1 mRNA levels by liver X receptor (LXR) and retinoid X receptor (RXR) agonists in cultured cells. Treatment of cells with indicated agonists is described in Materials and Methods. A: RAW264.7 cells: Northern blot (upper image) showing ABCG1 mRNA. Each lane contained RNA from a single triplicate plate of cells. Numbers at right refer to the estimated sizes (kb) of bands, determined from coelectrophoresed RNA standards. Lower image: cyclophilin A mRNA (cyc), approximately 0.75 kb, which was used for normalization; however, the ethidium-bromide-stained rRNA band intensities indicated more uniform lane loading. B: HepG2 cells: RT-PCR of ABCG1 cDNA derived by reverse transcription of HepG2 mRNA from cells treated in triplicate plates with indicated drugs. The expected amplicon size was 658 bp. Each lane represents amplification of cDNA derived from a single plate of cells. As positive controls, cDNA synthesized from human liver total RNA (Lv) and RNA from THP-1 macrophage cells treated with 20-hydroxycholesterol for 24 h (THP) were used as templates. The results shown are typical of six experiments performed with either of two primer pairs; however, with cDNA from cells treated with 9cRA alone, the expected amplicon was observed in 6 out of 18 reactions (not shown). C: Primary mouse hepatocytes: Upper image: Northern blot depicting ABCG1 mRNA; the autoradiogram was exposed for 2 weeks at −70°C. Abbreviation: T, T-0901317. Lower image: Cyclophilin A mRNA (cyc) for normalization. For this gel and blot, the cyclophilin A mRNA and rRNA band intensities were in agreement.

curacy ± 3 bases). No evidence of initiation at more-upstream sites was found; the antisense probe would have detected transcripts extending to base −661. On the basis of these concordant results, we conclude that the major promoter of the ABCG1 gene possesses multiple transcription start sites, the most upstream site at base −146 and the most common site at or around base −123, relative to translation initiation. These sites are 40 and 17 bases, respectively, farther upstream than the most upstream 5′ end of the major human ABCG1 mRNA transcript reported to date [GenBank accession BC029158, from Mammalian Gene Collection (61)]. The major start site found by us (−123) is consistent with that found by others for the mouse ABCG1 gene (12, 39), according to an alignment (UCSC Genome Browser) of the loosely conserved human and mouse sequences. We refer hereafter to the predominant start site as base +1 of exon 1;[2] the first base of the translation initiation codon would then be +124.

Identification of evolutionarily conserved putative LXREs

To identify sequences responsible for the marked responsiveness of the ABCG1 gene to oxysterols, we searched for putative LXREs that are evolutionarily conserved in human and mouse genomic sequences using the MatInspector and rVISTA programs, which employed nonidentical matrices and core definitions. Our search covered a 155,953-base region of the finished human chromosome 21 sequence (62), including 64,971 bases upstream from the major translation start site, all reported exons and introns of the ABCG1 gene, and 13,003 bases downstream from the last exon, as well as corresponding sequences near and within the mouse ABCG1 gene on chromosome 17 (51). We found two highly conserved putative LXREs that scored highly in both programs and a third that scored highly in only one program (**Fig. 3A**).

The first candidate LXRE, termed "LXRE-A" (Fig. 3B), is located in the first intron.[2] Its DR4 motif (MatInspector and rVISTA core/matrix scores 1.000/0.943 and 0.937/0.908, respectively) is located 1,247 bp downstream from the major transcription start site and in a region of ∼280 bp of sequence that is evolutionarily highly conserved in ABCG1 genes of mammals and, to a lesser extent, chicken. The DR4 bases are nearly identical in the first intron of the human, dog, mouse, and chicken ABCG1 genes (Fig. 3B), as well as in the ABCG1 orthologs of chimpanzee, cow, and laboratory opossum (*Monodelphis domestica*) (not shown). Potentially orthologous conserved sequences are found also in publicly available unassembled raw sequences of the genomes of rat, elephant, nine-banded armadillo (*Dasypus novemcinctus*), and duck-billed platypus (*Ornithorhynchus anatinus*) (not shown).

The second candidate LXRE, termed "LXRE-B" (Fig. 3C), is in the second intron, 14,500 bp downstream from the main transcription start site, in a small region (∼47 bp) of very high human/mouse conservation within a broader region (∼180 bp) of moderately conserved sequence. The DR4 motif (MatInspector and rVISTA scores 1.000/0.964 and 1.000/0.981, respectively) is highly conserved, except for the third and fourth inter-repeat bases,

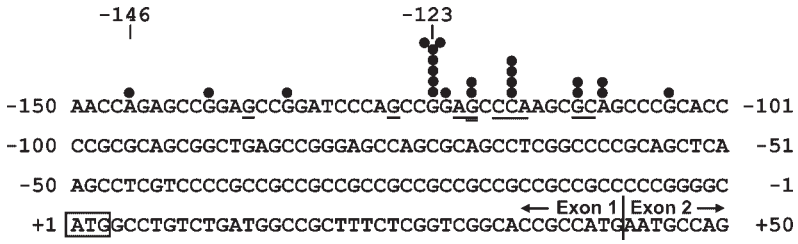

Fig. 2. Transcription start sites, 5′-untranslated region, and exon 1 of the major transcript of human ABCG1 gene. Bases are numbered with +1 defined as the A of the presumed translation start ATG (shown in box). Solid circles over bases identify 5′ ends of ABCG1 cDNA in clones obtained by 5′-rapid amplification of cDNA ends (RACE) of human placental cDNA. Each circle corresponds to one clone. Eight sequenced clones with apparent start sites downstream from −101 are not shown. The most upstream start site (base −146) and the apparently most common start (base −123) determined by 5′-RACE are numbered at top. Underlined bases are apparent transcription start sites determined by the RNase protection method (accuracy ± 3 bases). The double-underlined base is the apparently most prevalent start site (± 3 bases) as determined by the latter method.

in the second intron of the human, chimpanzee, dog, mouse, rat, chicken, and opossum ABCG1 orthologs. Surprisingly, it is also conserved in the compact second intron of a potentially orthologous ABCG1-like gene of the pufferfish *T. nigroviridis*.

A third candidate LXRE, termed "LXRE-C" (Fig. 3D), was found in a broad region of moderate sequence conservation in the second intron at 7,814 bp from the main transcription start site. It scored highly (1.000/0.886) in the rVISTA program but low (0.727/0.871) in the MatInspector program. Its DR4 sequence is conserved in the second intron of the human, chimpanzee, dog, mouse, rat, and cow ABCG1 genes; however, neighboring sequences on either side are less well conserved. In the chicken gene, the overall LXRE-C region appears to be less well conserved.

LXRE-A, -B, and -C differ from those previously reported for the human ABCG1 gene and located in the distal part of the second intron (40). The latter sequences are not conserved in rodent genomes and have lower MatInspector scores than those of LXRE-A and LXRE-B. In contrast, the mouse orthologs of LXRE-B and -C have recently been reported to confer LXR/RXR responsiveness to transfected test plasmids (12).

Lack of an LXRE in the promoter/upstream region

We tested the promoter/upstream region for a functional LXRE by transfecting into RAW264.7 cells plasmid constructs containing up to 4,793 bp of DNA upstream from the major transcription start site. As shown in **Fig. 4**, promoter/upstream sequences of 1,013 and 4,793 bp in length (constructs B, C) drove moderately strong expression of the reporter gene, compared with the promoterless pGL3-Basic vector (construct A) but did not confer responsiveness to T-0901317, as expected from our sequence analyses. Similar results were obtained with constructs containing between 244 and 2,033 bp of promoter/upstream sequence (data not shown). The construct with 1,013 bp of promoter sequence [pGL3-hABCG1(−1,013/+123), construct C] was subsequently used as a vector to assay the functionality of intronic sequences.

LXRE-A and LXRE-B are responsive to LXR agonist alone

To determine whether the LXRE-A, -B, and -C sequences are functionally active, we ligated segments of conserved sequences (287, 47, and 47 bp, respectively, termed "LXRE regions") containing the DR4 motifs and potentially important neighboring sequences into a site downstream (or in some cases upstream) from the reporter gene in pGL3-hABCG1(−1,013/+123) (Fig. 4, construct C). To perform this initial screen, mouse RAW264.7 macrophage cells were transfected with the individual constructs and subsequently treated with T-0901317.

The presence of the LXRE-A region, placed either downstream from the reporter gene or immediately upstream from the promoter, conferred strong responsiveness to T-0901317 (Fig. 4, constructs D–G). The degree of stimulation (3- to 5-fold) was independent of the position and orientation of the LXRE-A region relative to the promoter. Site-directed mutagenesis of the DR4 motif abolished the responsiveness of the LXRE-A region to T-0901317 (from 5- to 0.8-fold stimulation, construct H). Similar plasmid constructs containing the LXRE-B region downstream from the reporter gene in either orientation were highly responsive to LXR agonist treatment (Fig 4, constructs I, J). The 6- to 8-fold activation by LXRE-B was consistently higher than that by LXRE-A (comparing constructs I, J and D–G). Mutation of critical bases in the DR4 motif of the LXRE-B region in both the forward (construct K) and reverse (data not shown) orientations abolished the LXR responsiveness of these plasmid constructs. In contrast, a similar plasmid construct containing the LXRE-C region instead of LXRE-A or -B placed downstream from the reporter gene conferred little or no responsiveness to LXR agonist (construct L).

LXRE-A and LXRE-B are responsive to stimulation by LXR and/or RXR agonists in macrophage and hepatoma cells

In transfected RAW264.7 macrophage cells (**Fig. 5A**), the ABCG1 promoter in the absence of an LXRE was not stimulated by the LXR agonists 22-OH-cholesterol or T-0901317 alone, whereas the RXR agonist 9cRA, alone or in combi-

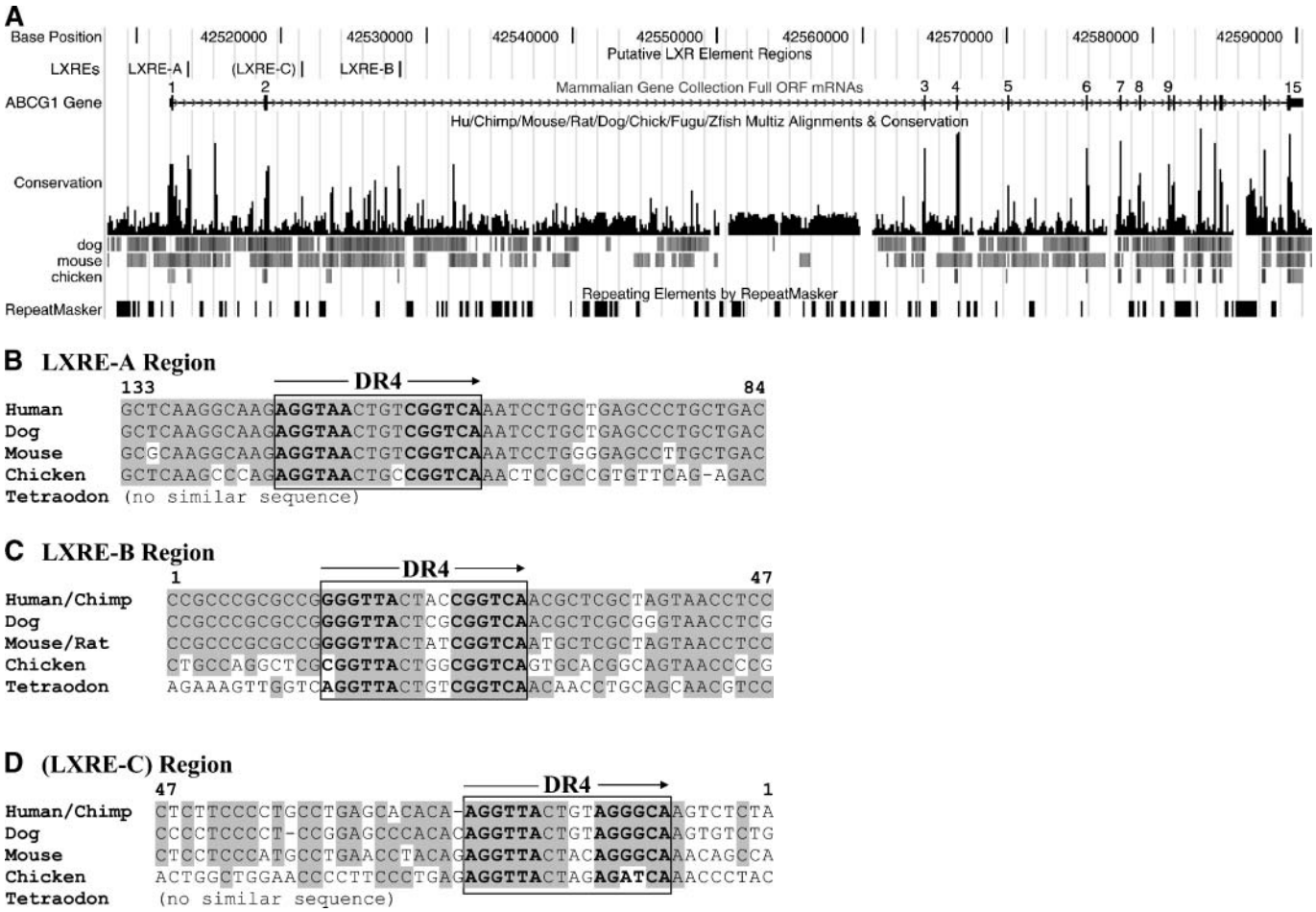

Fig. 3. Regions of evolutionarily conserved human genomic sequence containing putative LXR response elements (LXREs) in the human ABCG1 gene. A: Window from the UCSC Genome Browser (http://genome.ucsc.edu) showing the organization of the ABCG1 gene major transcript and putative LXRE positions in an 83 kbp region of the NCBI May 2004 assembly of the finished human genome (chr21: 42,508,000-42,591,000). Tracks from top to bottom are as follows: *1*) base position; *2*) putative LXREs (custom track); *3*) the positions of the 15 exons (numbered vertical bars) of the major transcript of human ABCG1 [GenBank accession BC029158]; *4*) a plot of evolutionary conservation among several species computed by the phastCons program ("windowing function" set to Mean); *5–7*) bands densities of similarity derived from Multiz alignments of draft genome sequences of dog (July 2004 freeze), mouse (May 2004 freeze), and chicken (February 2004 freeze); *8*) repetitive elements found by the RepeatMaster program. B–D: Putative LXRE regions of various species aligned by the Clustal W program (65). Sources of sequences are listed in Materials and Methods and below. To facilitate comparison, sequences are written in the direction in which the DR4 motifs follow the script RGGTYActnnMGKTCA; however, the numbers at the top of each alignment ascend in the centromeric-to-telomeric direction for the human ABCG1 gene. The DR4 hexanucleotide repeat bases are shown in boldface. Shaded bases are those found in at least three out of the four to five sequences shown in each panel. B: LXRE-A region in intron 1. The human sequence shown is chr21:42,513,542-42,513,599 and is bases 82–139 of a larger conserved region (287 bp, chr21:42,513,461-42,513,747) that was tested in transfection experiments. C: LXRE-B region in intron 2. The 47 bp sequence shown was tested in transfection experiments. The rat sequence is from the June 2003 assembly (which has a gap in the region of LXRE-A). The putative *Tetraodon* LXRE was found in the second intron of its apparent ABCG1 ortholog through the use of MatInspector; it did not align with mammalian sequences using the mVISTA and BLAST programs. D: LXRE-C region in intron 2. The 47 bp sequence shown for the human gene (chr21:42,521,372-42,521,418) and the 48 bp sequence shown for the mouse gene were tested in transfection experiments.

nation with LXR agonist, unexpectedly elicited up to 3-fold activation [first bar cluster, pGL3-hABCG1(−1,013/+123)]. A similar stimulation by 9cRA, however, was also observed in the promoterless pGL3-Basic vector (inset), indicating that the 9cRA stimulation of constructs lacking an LXRE is due to cryptic element(s) in the basic vector, rather than to the ABCG1 promoter. The LXRE-A region conferred the ability of LXR agonists and 9cRA separately to activate the ABCG1 promoter approximately 3-fold and 6-fold, respectively, and in combination, to synergistically activate it 16- to 18-fold (second bar cluster). The LXRE-A region mutated in the DR4 motif was unresponsive to LXR agonists with or without 9cRA (third bar cluster). The wild-type but not mutated LXRE-B region also conferred strong LXR responsiveness, but in a pattern different from that of LXRE-A and characterized by a stronger response to LXR agonist alone (6- to 8-fold) and a smaller, less than additive, enhancement by 9cRA, to achieve a maximum activation of 10- to 11.5-fold (fourth and fifth bar clusters).

We obtained similar but slightly divergent results with transfected HepG2 hepatoma cells (Fig. 5B). The intrinsic activity of the human ABCG1 promoter was consistently

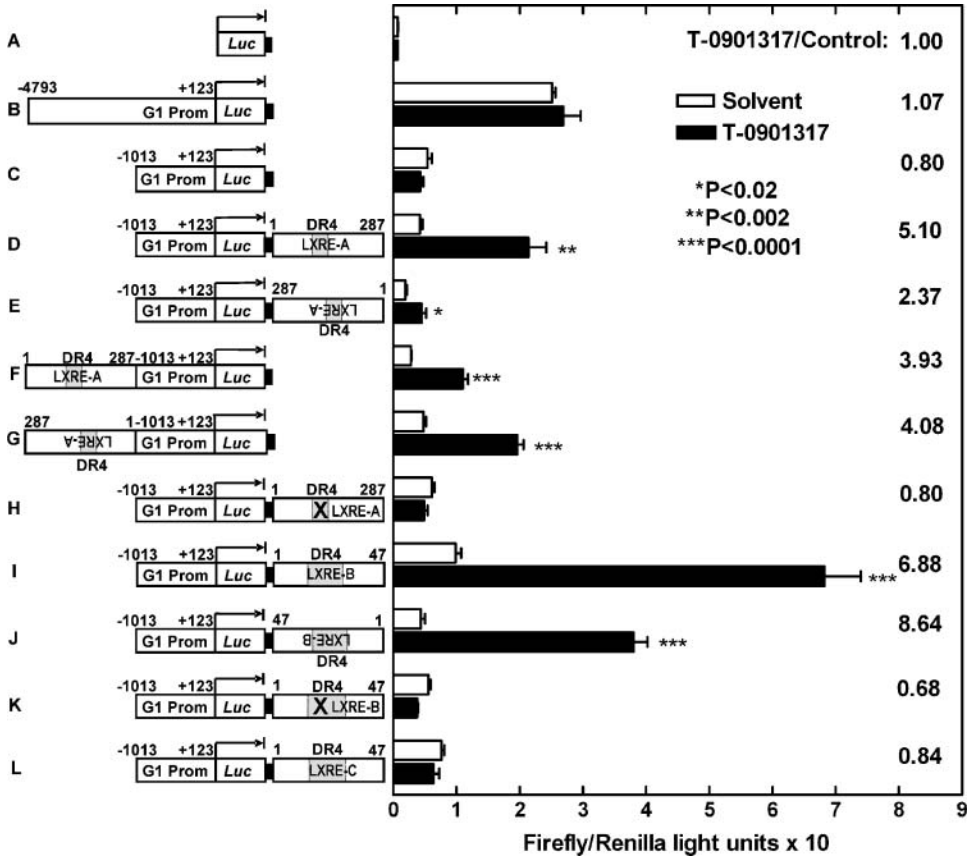

Fig. 4. LXR responsiveness of the ABCG1 promoter/upstream region and putative LXRE regions, determined by transfection of RAW264.7 cells. Plasmid constructs were constructed in the promoterless vector pGL3-Basic as described in Materials and Methods. At the left side are depicted important regions of the clones, drawn not to scale: the inserted promoter (G1 Prom, 1,013 bp of the major ABCG1 promoter plus 123 bp of the 5′-untranslated region), the firefly luciferase reporter gene (Luc), SV40 late polyadenylation signal (solid black box) of the vector, and tested ABCG1 intronic regions inserted either immediately downstream from polyadenylation signal in the *Sal*I site or immediately upstream from the promoter in the *Kpn*I site, in the orientation shown. The 287 bp LXRE-A, 47 bp LXRE-B, and 47 bp LXRE-C regions correspond to human genome positions listed in the legend for Fig. 3. The letter X indicates clones in which the DR4 sequence is mutated. The right side depicts normalized firefly luciferase activity (average of 4 wells ± SEM) for each construct and the relative stimulation by T-0901317. *P* values are based on comparison of the T-0901317-stimulated activity to the unstimulated activity for each construct. A plasmid with a very strong constitutive CMV promoter (pGL3-Control) was included in this experiment and had a normalized luciferase activity of 133 (data not shown). The data shown are from a single experiment representative of five experiments with similar results.

higher in HepG2 cells than in RAW264.7 cells. In HepG2 cells, the LXRE-A region conferred the ability of T-0901317 and 9cRA separately to activate the ABCG1 promoter 4.2-fold and 5.2-fold, respectively, and in combination, synergistically to activate it 18-fold (Fig. 5B, second bar cluster). Mutation of the DR4 of the LXRE-A region abolished responsiveness to LXR agonist with or without 9cRA (third bar cluster). In HepG2 cells, unlike in RAW264.7 cells, the presence of the wild-type LXRE-B region enhanced promoter activity approximately 3-fold in the absence of an added LXR agonist (fourth bar cluster). However, the addition of T-0901317 or 9cRA alone increased activity further by factors of 4.3 and 2.0, respectively. Mutations in the DR4 of the LXRE-B region led to a virtual loss of responsiveness to the LXR and RXR agonists (fifth bar cluster).

The activities of human and mouse LXRE-C were similarly tested in transfection experiments with RAW264.7 cells (Fig. 5C) and HepG2 cells (data not shown). Human LXRE-C was unresponsive to LXR agonist in the presence or absence of RXR agonist (Fig. 5C, third bar cluster), compared with the LXRE-A region tested in the same experiment (second bar cluster, 3.4- to 4.3-fold and 11-fold stimulation by LXR and LXR/RXR agonists, respectively). However, plasmids containing one copy of the mouse LXRE-C region were moderately responsive (fourth bar cluster, 1.8- to 3.0-fold and 4.0- to 5.1-fold stimulation by LXR and LXR/RXR agonists, respectively), and plasmids containing two tandem copies of the mouse LXRE-C region were highly responsive (fifth bar cluster, 11- to 14-fold and 33- to 35-fold stimulation by LXR and LXR/RXR agonists, respectively).

In conclusion, the human LXRE-A region and the human LXRE-B region confer robust responsiveness to LXR/RXR agonists. The LXRE-A region mediates a moderate response to LXR agonist alone and a very strong and syn-

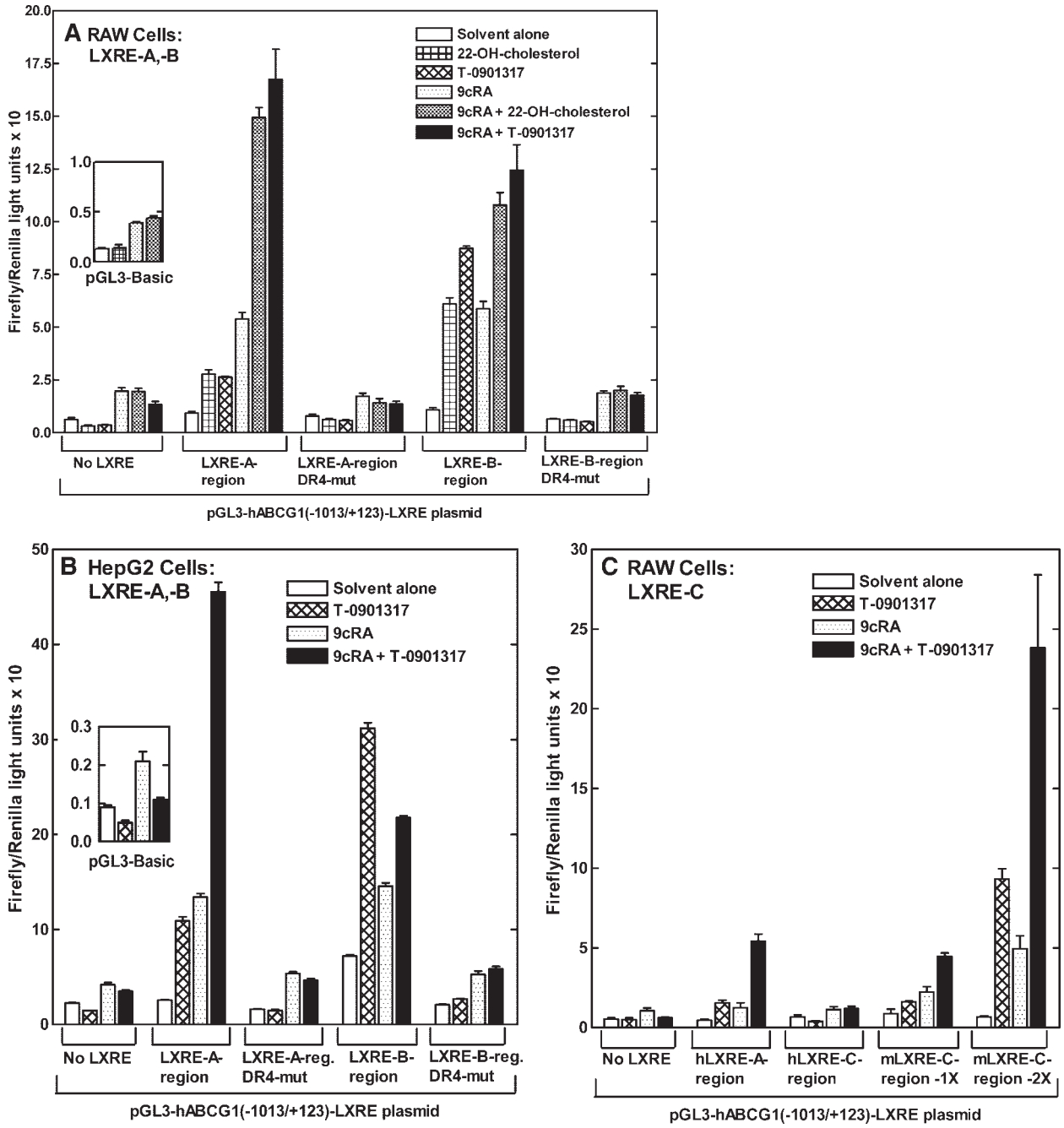

Fig. 5. Responsiveness of plasmid constructs containing LXRE regions to LXR and RXR agonists in RAW264.7 cells (A, C) and HepG2 cells (B). Plasmids containing tested human (h) and mouse (m) sequences downstream of the luciferase reporter gene were transfected as indicated. Cells were subsequently treated with 10 μM 22(*R*)-hydroxycholesterol, 1 μM T-0901317, and/or 10 μM 9cRA for 24 h as indicated. Firefly luciferase activities relative to *Renilla* luciferase light units from the cotransfected control plasmid are plotted (average of 4 wells ± SEM). Insert subpanels in A and B with magnified ordinate scales depict the activity of the empty vector pGL3-Basic and the consistently observed 2- to 3-fold stimulation of its activity by 9cRA in each cell type. A, B: Results comparing LXR responsiveness of human LXRE-A and -B and their respective DR4 mutants. C: Results comparing responsiveness of human LXRE-A to human and mouse LXRE-C containing one (1×) or two tandem (2×) copies. The data shown in A and B are from single experiments representative of five and two experiments with RAW264.7 and HepG2 cells, respectively. The data shown in panel C are representative of three experiments.

ergistic response to combined LXR + RXR agonists, whereas the LXRE-B region mediates a stronger response to LXR agonist alone, a response which is enhanced modestly, if at all, by the addition of RXR agonist. Although the human LXRE-C region appears to be essentially inactive, the mouse LXRE-C region is active.

Candidate LXREs are recognized by overexpressed LXR/RXR in cultured macrophage and hepatic cells

To further test whether LXR and RXR receptors recognize the candidate LXREs in cells, we measured responsiveness of the constructs containing LXRE regions when cotransfected with plasmids expressing LXR (α or β) and

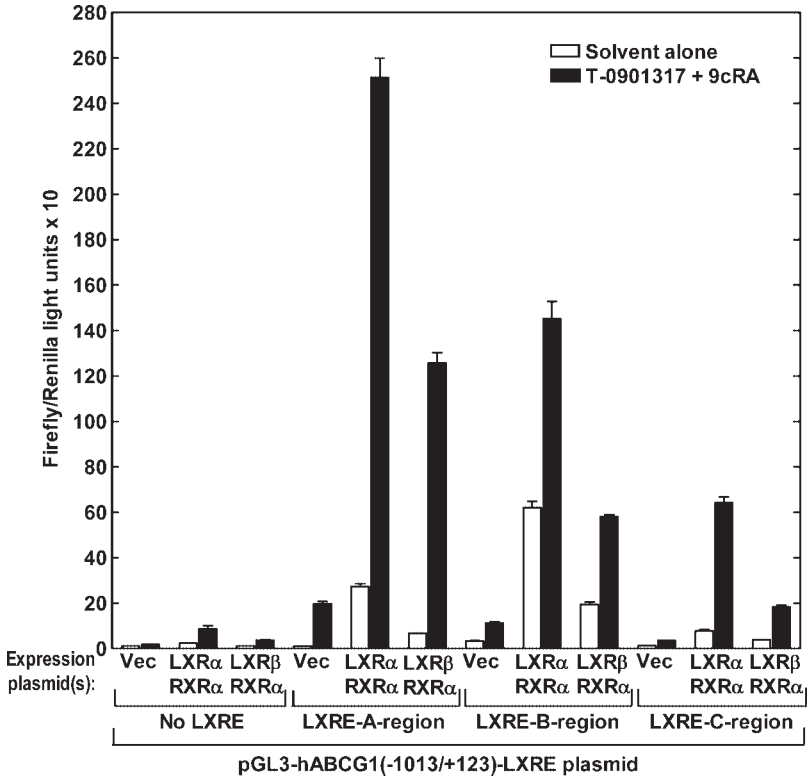

Fig. 6. LXR agonist responsiveness of plasmid constructs containing the ABCG1 promoter and LXRE regions in the presence of overexpressed LXR/RXR. HepG2 cells in 24-well plates were cotransfected with the indicated pGL-hABCG1(−1,013/+123) -LXRE constructs (0.5 μg/well) along with pcDNA-LXRα plus pcDNA-RXRα (0.05 μg/well each), pcDNA-LXRβ plus pcDNA-RXRα (0.05 μg/well each), or pcDNA3.1 vector (Vec, 0.1 μg/well), as indicated, as well as normalization plasmid pRL-SV40 (0.025 μg/well). LXR agonist (1 μM T-0901317) plus RXR agonist (10 μM 9cRA), and solvent alone (ethanol) were added as indicated. Normalized firefly luciferase activities (average of 4 wells ± SEM) are plotted. The data shown are from a single experiment representative of two experiments performed with HepG2 and one with RAW264.7 cells.

RXRα (**Fig. 6**). Basal and LXR/RXR agonist-stimulated luciferase expression from plasmid constructs containing the LXRE-A region or the LXRE-B region was very strongly enhanced by cotransfected LXRα/RXRα and, to a lesser extent, LXRβ/RXRα in HepG2 cells (Fig. 6, first three clusters of bars). The maximal overall activity of the promoter was achieved with the LXRE-A region in the presence of overexpressed LXRα/RXRα, whereas the maximal activity with the LXRE-B region and overexpressed LXRα/RXRα was approximately 60% of that with the LXRE-A region. Similar results were obtained with transfected RAW264.7 cells (data not shown). These results demonstrate that the human ABCG1 promoter is capable of very high activity when stimulated maximally by the LXR system acting through the LXRE sequences of this gene.

In contrast to its ineffectiveness in cells containing endogenous levels of receptors, the human LXRE-C region also conferred robust responsiveness to LXR agonist in the presence of cotransfected LXR/RXR, although to a lesser degree than that mediated by LXRE-A and LXRE-B (Fig. 6, fourth cluster of bars). These findings indicate that the LXRE-C region is capable of conferring some, albeit relatively weak, LXRE responsiveness when LXR/RXR receptor concentrations are high enough to activate transcription through suboptimal LXRE sequences.

Responsiveness of LXRE-A requires sequences neighboring the DR4 motif

Plasmid constructs containing the LXRE-A DR4 with few surrounding bases were found to be much less responsive to LXR agonist than was the well-conserved 287 bp LXRE-A region. To analyze the requirement for sequences neighboring the DR4, we prepared and tested a series of constructs that lack various segments of the 287 bp LXRE-A region, in which the DR4 motif is found at bases 106–121. As shown in **Fig. 7**, deletion of bases 128–287 (retaining 1–127) reduced responsiveness dramatically (from 13.5- to 2.0-fold). Removal of bases 1–75 alone (retaining 76–287) did not affect responsiveness. The highly truncated DR4-containing sequence 79–131 conferred only 1.8-fold stimulation by LXR/RXR agonists, and this response was further blunted when the DR4 motif was mutated. Some contribution of bases 235–287 to the maximal responsiveness was also found. We conclude that the overall LXRE-A region is a complex regulatory locus in which multiple regions are required for maximal LXR responsiveness. These regions contain several domains of high

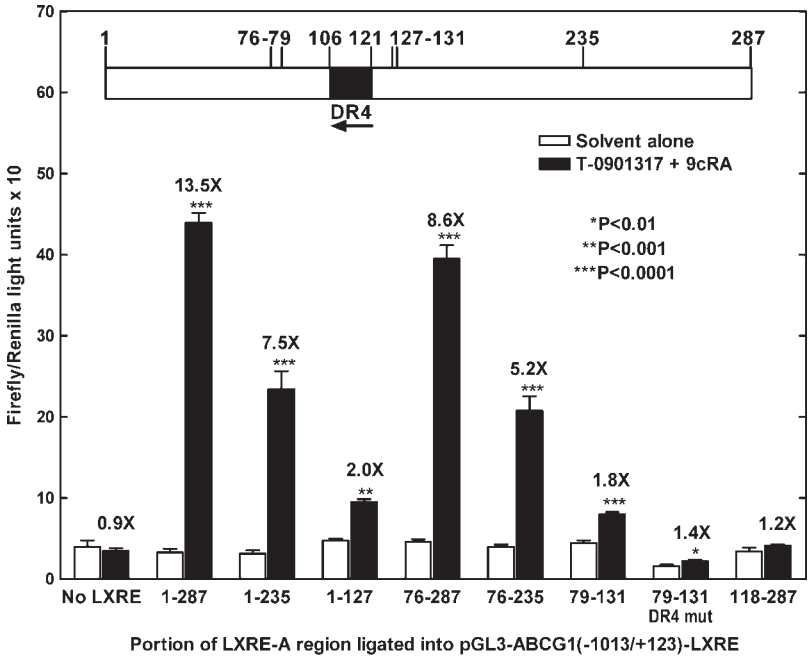

Fig. 7. Contribution of sequences neighboring the DR4 motif to the LXR responsiveness of LXRE-A region in transfected HepG2 cells. Cells were transfected with a series of pGL3-ABCG1 (−1,013/+123) with truncated LXRE-A region sequences ligated into the *Sal*I site, and activation of the reporter luciferase gene was measured after treatment with agonists, as indicated. The results shown (averages of 4 wells ± SEM) are from a single experiment and are representative of results obtained in five experiments with HepG2 and RAW264.7 cells. *P* values are based on the comparison of the agonist-stimulated activity to the unstimulated activity for each construct. The diagram at the top of the panel represents LXRE-A region (1–287) oriented (left to right) in the centromeric-to-telomeric direction, in contrast to the orientation shown in Fig. 3B. The numbers above each pair of bars are ratios of the activity in the presence of added agonists to that in the absence of added agonists, for each plasmid construct.

conservation in other mammalian genomes (alignments accessible on the UCSC Genome Browser).

LXRE-A and LXRE-B bind LXR and RXR in vitro and in vivo

To demonstrate that the DR4 elements of human LXRE-A and LXRE-B bind LXR/RXR heterodimers in cell-free systems, we performed electrophoretic mobility shift (gel shift) assays (EMSAs) with cell-free translated recombinant LXR and RXR proteins and short (28 bp) LXRE ^{32}P-labeled double-stranded probes. As shown in **Fig. 8A**, LXRα, LXRβ, or RXRα alone did not bind to either probe, while the combinations LXRα/RXRα and LXRβ/RXRα bound well to both. Thus the LXRE-A and LXRE-B sequences display the expected structural requirements for the heterodimerized receptors to form a stable complex. No strong preference of one paralog of LXR receptor for a particular LXRE was found. As expected, binding of LXR/RXR to ^{32}P-labeled LXRE-A and LXRE-B probes (28 bp) having mutated DR4 motifs was negligible compared with the wild-type probes (data not shown). Recombinant LXRα/RXRα and LXRβ/RXRα heterodimers also similarly bound ^{32}P-labeled 28 bp duplexes containing either the human or mouse LXRE-C motifs (data not shown).

The binding of cell-free translated LXRα/RXRα and LXRβ/RXRα heterodimers to LXRE-A and -B probes was blocked by a 30-fold (Fig. 8B) or 10-fold (data not shown) molar excess of nonradioactive oligonucleotide duplexes having either the same sequence as the probe or the sequence of the other LXRE. These results demonstrate that the LXRE-A and LXRE-B sequences bind to the same DNA binding site on the LXR/RXR heterodimers in this assay. In contrast, a 30-fold molar excess of LXRE-A or LXRE-B duplexes having sequences mutated in the same bases that were mutated for our transfection studies (Figs. 4, 5) failed to compete with the labeled LXRE-A or LXRE-B probes.

To perform chromatin immunoprecipitation experiments, we required an LXR antibody that can supershift natural LXR/RXR corepressor/coactivator complexes, in which epitope availability may differ from that in the cell-free translated LXR/RXR heterodimer. A screen of commercially available LXR antibodies using the gel shift assay revealed only one antibody that could supershift RAW264.7 nuclear protein complexes with short (28 bp) probes having LXRE-B and -C sequences (**Fig. 9A**, lanes 3–8, bands b and s) or the sequence of the known LXRE in the promoter of the human ABCA1 gene (36, 37) (data not shown). In contrast to LXRE-B and -C, a 28 bp LXRE-A probe bound to a faster migrating and nonsupershifted complex (lanes 1–2, band a). However a longer 50 bp LXRE-A probe (LXRE-A-50-centro) containing 28 bp upstream from the

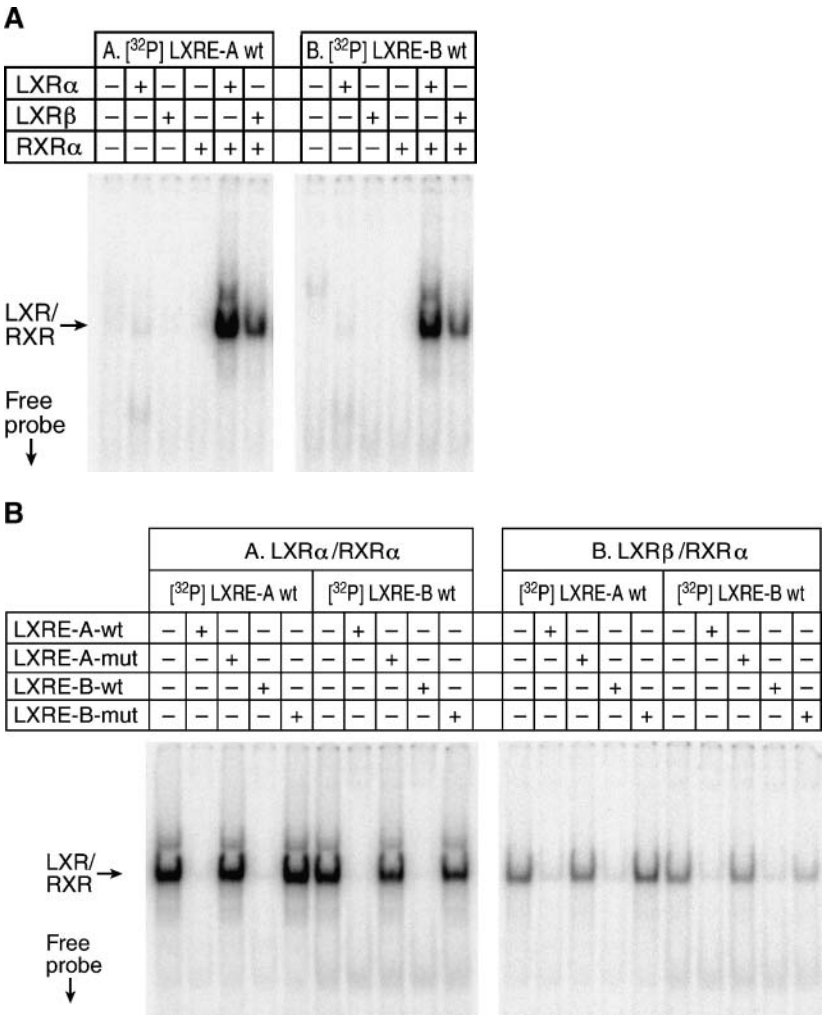

Fig. 8. Electrophoretic mobility shift assay (EMSA) demonstrating the binding of cell-free translated LXR and RXR proteins to DR4 sequences in putative LXREs of ABCG1. For each panel, gels A and B were run simultaneously. Each experiment shown was performed at least twice with similar results. A: Binding of LXRα, LXRβ, and RXRα and requirement for receptor heterodimerization. ^{32}P-end-labeled double-stranded probes (28 bp, described in Materials and Methods) consisted of the respective 16 bp DR4 regions and surrounding bases (six on each side) from LXRE-A (gel A) and LXRE-B (gel B). Receptors were provided by the addition of 1 μl LXR and/or 1 μl RXR transcription/translation (TNT) reaction mixtures, and/or sufficient template-minus reaction mixture to equalize the volume to 2 μl TNT mixture/tube, as indicated over each lane. The bands were supershifted by several antibodies (sc13068X, sc1591X, and sc-553X; Santa Cruz Biotechnology) against LXR and RXR (not shown). B: Competition of unlabeled duplexes with labeled LXRE probes for binding to cell-free transcribed/translated receptors. Reactions containing cell-free translated LXRα/RXRα proteins (gel A) or LXRβ/RXRα proteins (gel B) were carried out in the absence or presence of ~30-fold molar excess of unlabeled duplexes as indicated, which were added to the reaction mixtures prior to addition of the probe. The amounts of cell-free TNT mixtures added were as follows: 0.5 μl LXRα or 1 μl LXRβ, and 0.5 μl RXRα.

DR4 motif was able to form a more slowly migrating and supershiftable complex (lanes 11–12, bands b′ and s), indicating that the LXRE-A sequence, unlike the LXRE-B and -C sequences, requires bases farther from the DR4 core to bind the natural receptor complex in the EMSA. Similar results were obtained with THP-1 nuclear extracts (not shown).

Chromatin immunoprecipitation assays were performed to determine whether LXR and RXR are bound to the tested LXRE regions in nuclei of cells in which the ABCG1 gene is undergoing LXR-dependent transcriptional activation. For these studies, we used human THP-1 macrophage cells, in which ABCG1 mRNA is strongly and rapidly induced by treatment with LXR and RXR agonists in combination (39, 40) (unpublished observations). As shown in Fig. 9B, LXRE-A, -B, and -C-containing chromatin fragments from agonist-treated THP-1 cells were enriched by immunoprecipitation with anti-LXR (the same antibody that elicited supershifts shown in Fig. 9A) and anti-RXR. These results provide qualitative evidence that in living macrophage cells, LXR and RXR bind to the LXRE-A, -B, and -C sequences of the ABCG1 gene.

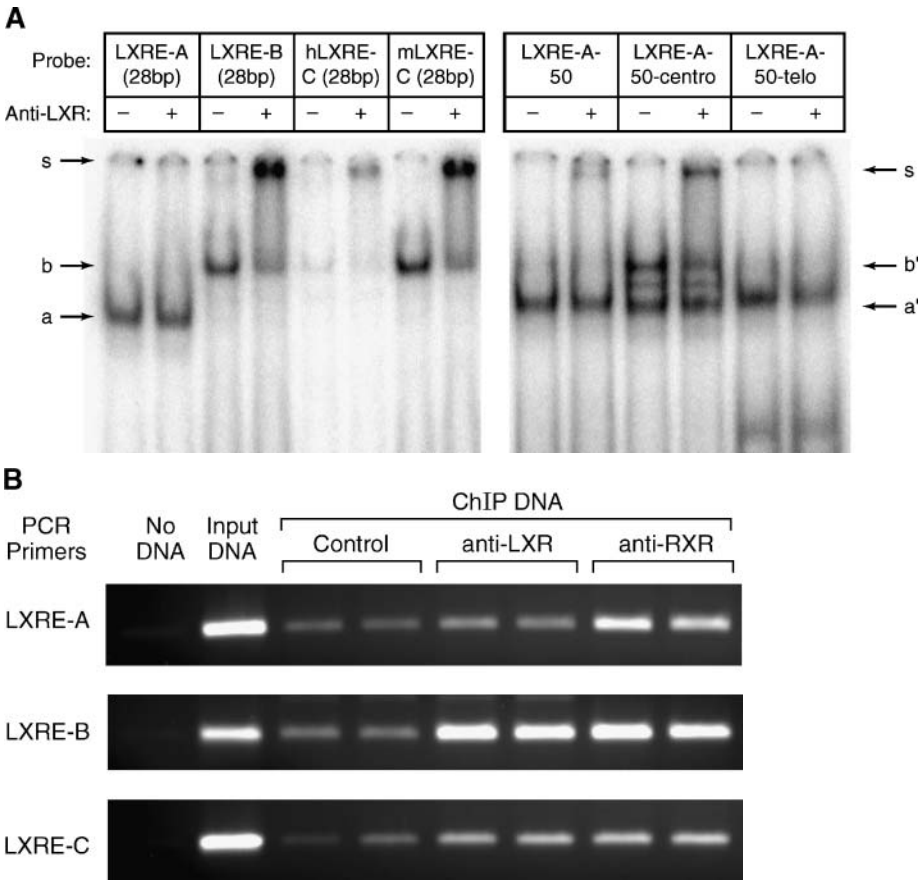

Fig. 9. A: EMSA demonstrating the binding of LXRE probes to RAW264.7 nuclear extract proteins. EMSA reactions contained indicated probes described in Materials and Methods. Anti-LXRα/β (4 μg, sc-1000X; Santa Cruz) was added where indicated and resulted in supershifted bands labeled s. Shifted bands labeled (a, b) and (a′, b′) were obtained with 28 bp and 50 bp probes, respectively. All probes were had similar specific radioactivities. B: Chromatin immunoprecipitation assays to detect binding of LXR/RXR to putative human ABCG1 LXREs. Differentiated THP-1 macrophages were treated with 1 μM T-0901317 and 5 μM 9cRA for 90 min. Fixed and sonicated chromatin was prepared and immunoprecipitated with nonimmune rabbit immunoglobulin G (control), anti-LXRα/β (Santa Cruz; sc-1000X), and anti-RXRα/β/γ (Santa Cruz; sc-774X), as described in Materials and Methods. Immunoprecipitated DNA was isolated and used as templates in duplicate PCR reactions with primers specific for LXRE-A, -B, and -C. Ethidium-bromide-stained amplicon bands (183, 164, and 170 bp, respectively) after 32 cycles (34 cycles for LXRE-B) are shown. Lanes marked "Input DNA" represent reactions containing DNA (5 ng) isolated from aliquots of chromatin removed prior to chromatin immunoprecipitation. These results are representative of those obtained with four immunoprecipitation experiments involving three different chromatin preparations.

DISCUSSION

The ABCG1 transporter is expressed in multiple tissues in which cholesterol transport and metabolism take place, including macrophages, liver, adipose tissue, and brain. In view of the potential role of ABCG1 in cholesterol trafficking and efflux (10–15), the identification of regulatory elements that modulate ABCG1 gene expression is important. The ABCG1 gene is noteworthy for its strong inducibility by LXR agonists such as hydroxycholesterols and T-0901317 and by lipid loading of cells by Ac-LDL, which activates the LXR system. The likelihood of an important function for ABCG1 in macrophages, where its gene is highly expressed, has been well appreciated, but ABCG1 may also play an important role in hepatocytes, where its mRNA levels can be strongly upregulated through the LXR system to levels that are likely to be functionally significant (Fig. 1C). Consistent with this proposal, Hoekstra et al. (9) reported that in rats, a high-cholesterol diet increased the ABCG1 mRNA abundance in hepatocytes 4-fold; because of the substantially greater abundance of hepatocytes relative to macrophages in liver, the contribution of these cells to total hepatic ABCG1 message was estimated to rise from 25% to 60%. Our findings provide a mechanistic explanation for this observation and suggest a potentially important role of hepatocyte ABCG1 in regulating cholesterol homeostasis.

Previous reports of LXREs in the mammalian ABCG1 gene have presented a confusing picture because of nonidentity of the proposed human and mouse LXREs and limitations of the string-search method used to detect them (12, 40). In this study, we performed an extensive search

for LXREs around and within the ABCG1 gene, taking note of previous reports of functional LXREs in introns of other genes (63, 64) and utilizing evolutionary conservation to assess potential functional importance of candidate sequences. We have identified two potential LXREs in the first two introns of the mammalian ABCG1 gene that are likely to be important loci of LXR regulation by virtue of satisfying three criteria: *i*) robust activity in cultured cells transfected with reporter plasmid constructs driven by the physiologically relevant ABCG1 promoter; *ii*) binding to LXR/RXR homodimers dependent on critical nucleotides in the DR4 motifs; and *iii*) evolutionary conservation in not only human and mouse, where LXR regulation of ABCG1 has been demonstrated (17), but also in other mammals and in chicken.

The two elements that we identified and characterized, LXRE-A and LXRE-B, are similar in that both confer strong LXR-agonist inducibility of the reporter gene when present on plasmid constructs in single copies and in the presence of endogenous levels of LXR and RXR in RAW264.7 and HepG2 cells (Figs. 4–6). However, LXRE-A and LXRE-B appear to differ in several respects. The first difference is that although the DR4 sequence of LXRE-B fits precisely a consensus sequence (rRGGTYActnnMGKTCA) of many LXREs, the DR4 of LXRE-A has an unusual A in base 5 of the first repeat. The second difference is in the reporter-gene responses to added LXR and RXR agonists. With LXRE-A, each type of agonist elicited significant but modest responses alone and a synergistically strong response when added together, whereas LXRE-B conferred a strong responsiveness to LXR agonist alone that was not strongly affected by added RXR agonist (Fig. 5). The third difference is that LXRE-A requires a larger expanse of neighboring bases than does LXRE-B for conferring robust LXR activation to the ABCG1 promoter (Fig. 7). This finding suggests that LXRE-A resides within an enhancer region more complex than that containing LXRE-B. Although the DR4 elements with only a few neighboring bases bind LXR/RXR heterodimers well in cell-free systems (Fig. 8A, B), sequences farther away are apparently required for proper binding of the LXREs to receptor-corepressor and -coactivator complexes (30, 32) and for the assembly of chromatin remodeling complexes.

The relative importance of the two LXREs in regulating the ABCG1 gene cannot be ascertained at present. On the one hand, LXRE-A may be more significant because its distance from the ABCG1 transcription start site (1,247 bp) is much less than that of LXRE-B (14,500 bp), and the maximal stimulation by LXR/RXR agonists is greater than that by LXRE-B in the cell lines tested (Figs. 5, 6). On the other hand, LXRE-B appears to be conserved over a greater evolutionary period than LXRE-A, and its greater distance from the ABCG1 promoter should not be prohibitively long (44). Probably both LXREs contribute, perhaps cooperatively, to the response of the endogenous gene.

LXRE-A and LXRE-B may also regulate the transcription of alternate human ABCG1 transcripts. Lorkowski et al. (39) identified transcripts in THP-1 monocytes that were initiated at a promoter ("promoter A") 19.3 kb upstream from the originally described promoter analyzed in this study ("promoter B"). Transcripts from both promoters were found to be strongly induced in THP-1 cells by treatment with LXR/RXR agonists, although the relative promoter usage was not determined. We confirmed these findings with both THP-1 and human spleen RNA using semiquantitative RT-PCR and found that promoter A usage is much less than promoter B usage in both tissues (data not shown). Because MatInspector analyses detected no high-scoring putative LXRE in the nonrepetitive sequence of a broad region around promoter A, we conclude that promoter A may be regulated through the same LXREs as those regulating promoter B.

After we completed most of our studies on human LXREs, Nakamura et al. (12) reported the identification of two LXRE sequences in the second intron of the mouse ABCG1 gene that were functional in HepG2 cells when tested with plasmids containing two tandem copies. These elements, termed "LXRE-6" and "LXRE-3," are orthologous to human LXRE-B and LXRE-C, respectively, in the present study. Our studies agree with Nakamura et al. regarding the robust activity of human LXRE-B/mouse LXRE-6, and extend their findings by demonstrating marked induction of the ABCG1 gene promoter by distantly placed native but not mutated LXRE-B in two physiologically relevant cell lines (Figs. 4, 5A). We also confirm their finding that the mouse LXRE-C confers LXR responsiveness. However, we found that the human LXRE-C region is nearly devoid of activity in transfection assays (Figs. 4, 5C) unless LXR and RXR are overexpressed (Fig. 6). Furthermore, in EMSA experiments with nuclear extracts, a human LXRE-C probe appears to bind much less complex supershifted with anti-LXR than does the analogous mouse LXRE-C probe. (Fig. 9A). Although the DR4 sequences of human and mouse LXRE-C are identical except for the noncritical third and fourth bases of the inter-repeat sequence, the bases surrounding the DR4 are not well conserved, particularly adjacent to the RXR binding region, where a potentially significant single-base deletion characterizes the chimp and human sequences when aligned to dog, rodent, and chicken sequences (Fig. 5D). We conclude that LXRE-A, which has not been reported previously, and LXRE-B are the probable major LXREs regulating the ABCG1 gene of humans and probably other mammals, whereas LXRE-C, which is less highly conserved and apparently stronger in mouse than in human, may contribute to regulation of the ABCG1 gene more in subprimate species than in primates.

Undiscovered but important LXREs may exist in the introns of other genes involved in reverse cholesterol transport and lipid metabolism. For example, introns 1 and 5 of the ABCA1 genes of human, mouse, and other mammals possess conserved DR4-like sequences very similar to those of LXRE-B of the ABCG1 gene.[3] It is interesting to

[3] These intronic putative LXRE sequences are located at chr9:104,768,568-104,768,583 and chr9:104,710,952-104,710,967 in the May 2004 human genome assembly (UCSC Genome Browser). The LXRE in the regulatory promoter of ABCA1 is located at chr9:104,770,045-104,770,060.

speculate that these elements may participate with the previously reported LXRE in the ABCA1 promoter (36, 37) to enhance or ensure LXR responsiveness. The possible existence of multiple, evolutionarily conserved, and functionally cooperative LXREs regulating both the ABCG1 and ABCA1 genes suggests that the LXR control of these genes is of great importance in the regulation of lipid and cholesterol homeostasis and for the survival of the organism.

This research was supported by the Intramural Research Program of the National Institutes of Health and the National Heart, Lung, and Blood Institute. The authors thank Marcelo Amar, Steve Demosky, and Federica Basso for the preparation and culture of mouse primary hepatocytes, Lita Freeman for the isolation and Northern analysis of hepatocyte RNA, Toshi Ito for the mouse ABCG1 cDNA probe and for help with preparing the ABCG1 promoter, Lita Freeman and Cathy Knapper for expert advice, and Manny Duarte for technical assistance.

REFERENCES

1. Dean, M., A. Rzhetsky, and R. Allikmets. 2001. The human ATP-binding cassette (ABC) transporter superfamily. *Genome Res.* **11:** 1156–1166.
2. Dean, M., Y. Hamon, and G. Chimini. 2001. The human ATP-binding cassette (ABC) transporter superfamily. *J. Lipid Res.* **42:** 1007–1017.
3. Savary, S., F. Denizot, M. Luciani, M. Mattei, and G. Chimini. 1996. Molecular cloning of a mammalian ABC transporter homologous to Drosophila white gene. *Mamm. Genome.* **7:** 673–676.
4. Chen, H., C. Rossier, M. D. Lalioti, A. Lynn, A. Chakravarti, G. Perrin, and S. E. Antonarakis. 1996. Cloning of the cDNA for a human homologue of the Drosophila white gene and mapping to chromosome 21q22.3. *Am. J. Hum. Genet.* **59:** 66–75.
5. Croop, J. M., G. E. Tiller, J. A. Fletcher, M. L. Lux, E. Raab, D. Goldenson, D. Son, S. Arciniegas, and R. L. Wu. 1997. Isolation and characterization of a mammalian homolog of the Drosophila white gene. *Gene.* **185:** 77–85.
6. Cserepes, J., Z. Szentpetery, L. Seres, C. Ozvegy-Laczka, T. Langmann, G. Schmitz, H. Glavinas, I. Klein, L. Homolya, A. Varadi, et al. 2004. Functional expression and characterization of the human ABCG1 and ABCG4 proteins: indications for heterodimerization. *Biochem. Biophys. Res. Commun.* **320:** 860–867.
7. Su, Y. R., M. F. Linton, and S. Fazio. 2002. Rapid quantification of murine ABC mRNAs by real time reverse transcriptase-polymerase chain reaction. *J. Lipid Res.* **43:** 2180–2187.
8. Langmann, T., R. Mauerer, A. Zahn, C. Moehle, M. Probst, W. Stremmel, and G. Schmitz. 2003. Real-time reverse transcription-PCR expression profiling of the complete human ATP-binding cassette transporter superfamily in various tissues. *Clin. Chem.* **49:** 230–238.
9. Hoekstra, M., J. K. Kruijt, M. Van Eck, and T. J. Van Berkel. 2003. Specific gene expression of ATP-binding cassette transporters and nuclear hormone receptors in rat liver parenchymal, endothelial, and Kupffer cells. *J. Biol. Chem.* **278:** 25448–25453.
10. Klucken, J., C. Buchler, E. Orso, W. E. Kaminski, M. Porsch-Ozcurumez, G. Liebisch, M. Kapinsky, W. Diederich, W. Drobnik, M. Dean, et al. 2000. ABCG1 (ABC8), the human homolog of the Drosophila white gene, is a regulator of macrophage cholesterol and phospholipid transport. *Proc. Natl. Acad. Sci. USA.* **97:** 817–822.
11. Wang, N., D. Lan, W. Chen, F. Matsuura, and A. R. Tall. 2004. ATP-binding cassette transporters G1 and G4 mediate cellular cholesterol efflux to high-density lipoproteins. *Proc. Natl. Acad. Sci. USA.* **101:** 9774–9779.
12. Nakamura, K., M. A. Kennedy, A. Baldan, D. D. Bojanic, K. Lyons, and P. A. Edwards. 2004. Expression and regulation of multiple murine ATP-binding cassette transporter G1 mRNAs/isoforms that stimulate cellular cholesterol efflux to high density lipoprotein. *J. Biol. Chem.* **279:** 45980–45989.
13. Ito, T., S. L. Sabol, M. Amar, C. Knapper, C. Duarte, R. D. Shamburek, S. Meyn, S. Santamarina-Fojo, and H. B. Brewer. 2000. Adenovirus-mediated expression establishes an in vivo role for human ABCG1 (ABC8) in lipoprotein metabolism. *Circulation.* **102:** 1525.
14. Ito, T. 2003. Physiological function of ABCG1. *Drug News Perspect.* **16:** 490–492.
15. Neufeld, E. B., S. Sabol, A. T. Remaley, T. Ito, S. J. Demosky, J. Stonik, S. Santamarina-Fojo, and H. B. Brewer. 2001. Cellular localization and trafficking of human ABCG1. *Circulation.* **104:** 708.
16. Brewer, H. B., Jr., and S. Santamarina-Fojo. 2003. New insights into the role of the adenosine triphosphate-binding cassette transporters in high-density lipoprotein metabolism and reverse cholesterol transport. *Am. J. Cardiol.* **91:** 3E–11E.
17. Venkateswaran, A., J. J. Repa, J. M. Lobaccaro, A. Bronson, D. J. Mangelsdorf, and P. A. Edwards. 2000. Human white/murine ABC8 mRNA levels are highly induced in lipid-loaded macrophages. A transcriptional role for specific oxysterols. *J. Biol. Chem.* **275:** 14700–14707.
18. Fu, X., J. G. Menke, Y. Chen, G. Zhou, K. L. MacNaul, S. D. Wright, C. P. Sparrow, and E. G. Lund. 2001. 27-Hydroxycholesterol is an endogenous ligand for liver X receptor in cholesterol-loaded cells. *J. Biol. Chem.* **276:** 38378–38387.
19. Repa, J. J., S. D. Turley, J. A. Lobaccaro, J. Medina, L. Li, K. Lustig, B. Shan, R. A. Heyman, J. M. Dietschy, and D. J. Mangelsdorf. 2000. Regulation of absorption and ABC1-mediated efflux of cholesterol by RXR heterodimers. *Science.* **289:** 1524–1529.
20. Venkateswaran, A., B. A. Laffitte, S. B. Joseph, P. A. Mak, D. C. Wilpitz, P. A. Edwards, and P. Tontonoz. 2000. Control of cellular cholesterol efflux by the nuclear oxysterol receptor LXR alpha. *Proc. Natl. Acad. Sci. USA.* **97:** 12097–12102.
21. Tontonoz, P., and D. J. Mangelsdorf. 2003. Liver X receptor signaling pathways in cardiovascular disease. *Mol. Endocrinol.* **17:** 985–993.
22. Willy, P. J., K. Umesono, E. S. Ong, R. M. Evans, R. A. Heyman, and D. J. Mangelsdorf. 1995. LXR, a nuclear receptor that defines a distinct retinoid response pathway. *Genes Dev.* **9:** 1033–1045.
23. Janowski, B. A., P. J. Willy, T. R. Devi, J. R. Falck, and D. J. Mangelsdorf. 1996. An oxysterol signalling pathway mediated by the nuclear receptor LXR alpha. *Nature.* **383:** 728–731.
24. Edwards, P. A., H. R. Kast, and A. M. Anisfeld. 2002. BAREing it all: the adoption of LXR and FXR and their roles in lipid homeostasis. *J. Lipid Res.* **43:** 2–12.
25. Schultz, J. R., H. Tu, A. Luk, J. J. Repa, J. C. Medina, L. Li, S. Schwendner, S. Wang, M. Thoolen, D. J. Mangelsdorf, et al. 2000. Role of LXRs in control of lipogenesis. *Genes Dev.* **14:** 2831–2838.
26. Mangelsdorf, D. J., and R. M. Evans. 1995. The RXR heterodimers and orphan receptors. *Cell.* **83:** 841–850.
27. Willy, P. J., and D. J. Mangelsdorf. 1997. Unique requirements for retinoid-dependent transcriptional activation by the orphan receptor LXR. *Genes Dev.* **11:** 289–298.
28. Steffensen, K. R., and J. A. Gustafsson. 2004. Putative metabolic effects of the liver X receptor (LXR). *Diabetes.* **53 (Suppl. 1):** 36–42.
29. Peet, D. J., B. A. Janowski, and D. J. Mangelsdorf. 1998. The LXRs: a new class of oxysterol receptors. *Curr. Opin. Genet. Dev.* **8:** 571–575.
30. Hu, X., S. Li, J. Wu, C. Xia, and D. S. Lala. 2003. Liver X receptors interact with corepressors to regulate gene expression. *Mol. Endocrinol.* **17:** 1019–1026.
31. Wagner, B. L., A. F. Valledor, G. Shao, C. L. Daige, E. D. Bischoff, M. Petrowski, K. Jepsen, S. H. Baek, R. A. Heyman, M. G. Rosenfeld, et al. 2003. Promoter-specific roles for liver X receptor/corepressor complexes in the regulation of ABCA1 and SREBP1 gene expression. *Mol. Cell. Biol.* **23:** 5780–5789.
32. Huuskonen, J., P. E. Fielding, and C. J. Fielding. 2004. Role of p160 coactivator complex in the activation of liver X receptor. *Arterioscler. Thromb. Vasc. Biol.* **24:** 703–708.
33. Tangirala, R. K., E. D. Bischoff, S. B. Joseph, B. L. Wagner, R. Walczak, B. A. Laffitte, C. L. Daige, D. Thomas, R. A. Heyman, D. J. Mangelsdorf, et al. 2002. Identification of macrophage liver X receptors as inhibitors of atherosclerosis. *Proc. Natl. Acad. Sci. USA.* **99:** 11896–11901.
34. Ulven, S. M., K. T. Dalen, J. A. Gustafsson, and H. I. Nebb. 2004. Tissue-specific autoregulation of the LXRalpha gene facilitates induction of apoE in mouse adipose tissue. *J. Lipid Res.* **45:** 2052–2062.

35. Quinet, E. M., D. A. Savio, A. R. Halpern, L. Chen, C. P. Miller, and P. Nambi. 2004. Gene-selective modulation by a synthetic oxysterol ligand of the liver X receptor. *J. Lipid Res.* **45:** 1929–1942.
36. Schwartz, K., R. M. Lawn, and D. P. Wade. 2000. ABC1 gene expression and ApoA-I-mediated cholesterol efflux are regulated by LXR. *Biochem. Biophys. Res. Commun.* **274:** 794–802.
37. Costet, P., Y. Luo, N. Wang, and A. R. Tall. 2000. Sterol-dependent transactivation of the ABC1 promoter by the liver X receptor/retinoid X receptor. *J. Biol. Chem.* **275:** 28240–28245.
38. Langmann, T., M. Porsch-Ozcurumez, U. Unkelbach, J. Klucken, and G. Schmitz. 2000. Genomic organization and characterization of the promoter of the human ATP-binding cassette transporter-G1 (ABCG1) gene. *Biochim. Biophys. Acta.* **1494:** 175–180.
39. Lorkowski, S., S. Rust, T. Engel, E. Jung, K. Tegelkamp, E. A. Galinski, G. Assmann, and P. Cullen. 2001. Genomic sequence and structure of the human ABCG1 (ABC8) gene. *Biochem. Biophys. Res. Commun.* **280:** 121–131.
40. Kennedy, M. A., A. Venkateswaran, P. T. Tarr, I. Xenarios, J. Kudoh, N. Shimizu, and P. A. Edwards. 2001. Characterization of the human ABCG1 gene: liver X receptor activates an internal promoter that produces a novel transcript encoding an alternative form of the protein. *J. Biol. Chem.* **276:** 39438–39447.
41. Schmitz, G., T. Langmann, and S. Heimerl. 2001. Role of ABCG1 and other ABCG family members in lipid metabolism. *J. Lipid Res.* **42:** 1513–1520.
42. Margulies, E. H., M. Blanchette, D. Haussler, and E. D. Green. 2003. Identification and characterization of multi-species conserved sequences. *Genome Res.* **13:** 2507–2518.
43. Dermitzakis, E. T., A. Reymond, R. Lyle, N. Scamuffa, C. Ucla, S. Deutsch, B. J. Stevenson, V. Flegel, P. Bucher, C. V. Jongeneel, et al. 2002. Numerous potentially functional but non-genic conserved sequences on human chromosome 21. *Nature.* **420:** 578–582.
44. Nobrega, M. A., I. Ovcharenko, V. Afzal, and E. M. Rubin. 2003. Scanning human gene deserts for long-range enhancers. *Science.* **302:** 413.
45. Carey, M., and S. T. Smale. 2000. Transcriptional Regulation in Eukaryotes. Cold Spring Harbor Laboratory Press, Cold Spring Harbor, NY. 124–125.
46. Mayor, C., M. Brudno, J. R. Schwartz, A. Poliakov, E. M. Rubin, K. A. Frazer, L. S. Pachter, and I. Dubchak. 2000. VISTA: visualizing global DNA sequence alignments of arbitrary length. *Bioinformatics.* **16:** 1046–1047.
47. Couronne, O., A. Poliakov, N. Bray, T. Ishkhanov, D. Ryaboy, E. Rubin, L. Pachter, and I. Dubchak. 2003. Strategies and tools for whole-genome alignments. *Genome Res.* **13:** 73–80.
48. Quandt, K., K. Frech, H. Karas, E. Wingender, and T. Werner. 1995. MatInd and MatInspector: new fast and versatile tools for detection of consensus matches in nucleotide sequence data. *Nucleic Acids Res.* **23:** 4878–4884.
49. Loots, G. G., I. Ovcharenko, L. Pachter, I. Dubchak, and E. M. Rubin. 2002. rVista for comparative sequence-based discovery of functional transcription factor binding sites. *Genome Res.* **12:** 832–839.
50. International Human Genome Sequencing Consortium. 2004. Finishing the euchromatic sequence of the human genome. *Nature.* **431:** 931–945.
51. Waterston, R. H., and Mouse Genome Sequencing Consortium. 2002. Initial sequencing and comparative analysis of the mouse genome. *Nature.* **420:** 520–562.
52. Gibbs, R. A., and Rat Genome Sequencing Project Consortium. 2004. Genome sequence of the Brown Norway rat yields insights into mammalian evolution. *Nature.* **428:** 493–521.
53. International Chicken Genome Sequencing Consortium. 2004. Sequence and comparative analysis of the chicken genome provide unique perspectives on vertebrate evolution. *Nature.* **432:** 695–716.
54. Jaillon, O., J. M. Aury, F. Brunet, J. L. Petit, N. Stange-Thomann, E. Mauceli, L. Bouneau, C. Fischer, C. Ozouf-Costaz, A. Bernot, et al. 2004. Genome duplication in the teleost fish Tetraodon nigroviridis reveals the early vertebrate proto-karyotype. *Nature.* **431:** 946–957.
55. Kent, W. J., C. W. Sugnet, T. S. Furey, K. M. Roskin, T. H. Pringle, A. M. Zahler, and D. Haussler. 2002. The human genome browser at UCSC. *Genome Res.* **12:** 996–1006.
56. Karolchik, D., R. Baertsch, M. Diekhans, T. S. Furey, A. Hinrichs, Y. T. Lu, K. M. Roskin, M. Schwartz, C. W. Sugnet, D. J. Thomas, et al. 2003. The UCSC genome browser database. *Nucleic Acids Res.* **31:** 51–54.
57. Shinar, D. M., N. Endo, S. J. Rutledge, R. Vogel, G. A. Rodan, and A. Schmidt. 1994. NER, a new member of the gene family encoding the human steroid hormone nuclear receptor. *Gene.* **147:** 273–276.
58. Mangelsdorf, D. J., E. S. Ong, J. A. Dyck, and R. M. Evans. 1990. Nuclear receptor that identifies a novel retinoic acid response pathway. *Nature.* **345:** 224–229.
59. Dignam, J. D., R. M. Lebovitz, and R. G. Roeder. 1983. Accurate transcription initiation by RNA polymerase II in a soluble extract from isolated mammalian nuclei. *Nucleic Acids Res.* **11:** 1475–1489.
60. Kaplan, R., X. Gan, J. G. Menke, S. D. Wright, and T. Q. Cai. 2002. Bacterial lipopolysaccharide induces expression of ABCA1 but not ABCG1 via an LXR-independent pathway. *J. Lipid Res.* **43:** 952–959.
61. Strausberg, R. L., E. A. Feingold, R. D. Klausner, and F. S. Collins. 1999. The mammalian gene collection. *Science.* **286:** 455–457.
62. Hattori, M., and Chromosome 21 Mapping and Sequencing Consortium. 2000. The DNA sequence of human chromosome 21. *Nature.* **405:** 311–319.
63. Laffitte, B. A., J. J. Repa, S. B. Joseph, D. C. Wilpitz, H. R. Kast, D. J. Mangelsdorf, and P. Tontonoz. 2001. LXRs control lipid-inducible expression of the apolipoprotein E gene in macrophages and adipocytes. *Proc. Natl. Acad. Sci. USA.* **98:** 507–512.
64. Zhang, Y., J. J. Repa, K. Gauthier, and D. J. Mangelsdorf. 2001. Regulation of lipoprotein lipase by the oxysterol receptors, LXRalpha and LXRbeta. *J. Biol. Chem.* **276:** 43018–43024.
65. Thompson, J. D., D. G. Higgins, and T. J. Gibson. 1994. CLUSTAL W: improving the sensitivity of progressive multiple sequence alignment through sequence weighting, position-specific gap penalties and weight matrix choice. *Nucleic Acids Res.* **22:** 4673–4680.